Hindawi
Complexity
Volume 2022, Article ID 7903450, 18 pages
https://doi.org/10.1155/2022/7903450

Research Article

A State-Dependent Impulsive Nonlinear System with Ratio-Dependent Action Threshold for Investigating the Pest-Natural Enemy Model

Ihsan Ullah Khan,[1] Saif Ullah,[2,3] Ebenezer Bonyah,[4] Basem Al Alwan,[5] and Ahmed Alshehri[6]

[1]*Department of Mathematics, Institute of Numerical Sciences, Gomal University, Dera Ismail Khan 29050, KPK, Pakistan*
[2]*Department of Mathematics, University of Peshawar, Peshawar, Pakistan*
[3]*Department of Mathematics, Faculty of Science and Technology, Universitas Airlangga, Surabaya 60115, Indonesia*
[4]*Department of Mathematics Education, Akenten Appiah Menka University of Skills Training and Entrepreneurial Development, Kumasi, Ghana*
[5]*Chemical Engineering Department, College of Engineering, King Khalid University, Abha 61411, Saudi Arabia*
[6]*Department of Mathematics, Faculty of Sciences, King Abdulaziz University, Jeddah 21589, Saudi Arabia*

Correspondence should be addressed to Ebenezer Bonyah; ebbonya@gmail.com

Received 20 September 2021; Accepted 17 December 2021; Published 18 January 2022

Academic Editor: George V. Popescu

Based on the Lotka–Volterra system, a pest-natural enemy model with nonlinear feedback control as well as nonlinear action threshold is introduced. The model characterizes the implementation of comprehensive prevention and control measures when the pest density reaches the nonlinear action threshold level depending on the pest density and its change rate. The mortality rate of the pest is a saturation function that strictly depends on their density while the release of natural enemies is also a nonlinear pulse term depending on the density of real-time natural enemies. The exact impulsive and phase sets are given. The definition and properties of the Poincaré map corresponding to the pulse points on the phase set are provided. We investigate the existence and stability of boundary and interior order-1 periodic solution. The theoretical analysis developed in the present paper combined with nonlinear controlling measures as well as nonlinear action threshold methods and techniques laid the foundation for the establishment and analysis of other state-dependent feedback control models.

1. Introduction

Pest control [1–6] is not only an ancient problem but also a new challenge faced by the modern world. Various scientific and effective methods [7–13] are needed to comprehensively prevent and control pest outbreaks and reinfestation. The most common early method was chemical control [14, 15], that is, the method of controlling pest by spraying pesticides during pest outbreaks. The main advantages of chemical control are quick effect and convenient use. It can eradicate or maintain the number of pests at a lower level within a short period of time. Therefore, chemical control is still one of the important means to control pest population. Biological control [16–18] is another important control method, which has the advantages of strong effect and long duration, and is also an environmental friendly control method. Maiti et al. [19] used a valuable technique known as sterile insect release method (SIRM) to manage the pest population. The authors discussed the effect of uncertain ecological variations on sterile and fertile insects. Other main methods are physical control and agricultural control. For example, the agricultural control method is a method to reduce or control pests through measures such as crop rotation, intercropping, and reasonable adjustment of cultivation procedures.

Each pest control method has its advantages and disadvantages. Due to long-term and high-dose use, pests can easily develop resistance to specific pesticides, resulting in pest control failure and pest reemergance. However, other control strategies cannot effectively reduce the number of pests in a short time because of their slow effectiveness. Therefore, how to effectively and reasonably use multiple methods is the best choice for pest control. Based on this, the Food and Agriculture Organization of the United Nations (FAO) proposed the concept of integrated pest management (IPM) [1, 20, 21] and defined it as follows: "IPM is a pest control system that comprehensively considers the population dynamics of the pest and its related environment and uses all appropriate control techniques and methods that work as closely as possible to maintain levels at which pest populations do not cause economic harm." Both experimentally [22, 23] and theoretically [24, 25], it has been proved that IPM is more practical than the classic approach. This is one of the most useful methods which minimizes damage to individuals and the environment in addressing pest control.

In this perspective, researchers have studied the mathematical problems based on impulsive differential equations in order investigate the dynamics of IPM and compass biped robotic systems. In numerous realistic problems, impulses often occur at state-dependent. Therefore, it is more feasible to apply the procedure of state-dependent feedback control to model real-world issues. Znegui et al. [26] used an impulsive hybrid nonlinear system to construct a passive biped robot model that demonstrates complicated behaviors. In [27], the authors constructed a Poincaré map which was further utilized to examine the existence and stability of order-1 periodic type solution of the problem under consideration. Many new systems on the design of specific analytical expression of the hybrid state-dependent Poincaré were studied in [28, 29]. The authors in [26–29] portrayed an expression of the controlled Poincaré map to discuss the stabilization of passive dynamic walking of the compass-gait biped robot. The compass-gait biped robot is a two-DoF legged mechanical system which is identified by its passive dynamic walking. The one-DoF mechanical systems are also of great importance. Some articles related to one-DoF state-feedback control with respect to different perspectives can be found in [30, 31].

The impulsive differential equations are also used proficiently in epidemic dynamics [32] and population dynamics [33–35]. A basic assumption of the above series of studies is that regardless of how huge the number of pests or the growth rate is, as long as the number of pest populations touches economic threshold (ET) [33–35], the IPM strategy can be implemented. However, there are two basic situations of actual pest growth that require high attention: first, the number of pests is comparatively large, and the rate of change is small; second, the population is small, but the rate of change is high. A fundamental problem illustrated by these two situations is that when the pest population is large (such as exceeding ET), the growth rate is small or even negative at this time. In this case, even if the IPM strategy is not implemented, the number of pests may not exceed economic injury level (EIL) [36]. Another situation is that the number of pests is not large, and the rate at which the pest population is growing is very large. In this case, if the control strategy is not implemented in time, it may lead to a large outbreak of pests. Next, in order to establish appropriate and effective integrated controlling strategies, the IPM process needs precise inspection of the pest quantity. The mortality rate should be fluctuated according to the saturating function which relies upon the density of pest, and the releasing quantity of natural enemies should be a function of their density. Therefore, keeping in mind the above factors, a feasible new state-feedback control pest-natural enemy ecosystem with nonlinear controlling measures as well as nonlinear action threshold system is proposed. The corresponding analytical techniques and numerical methods are developed to examine the dynamical aspects of the system under consideration.

The main research contents are reflected in the following aspects. We construct a Lotka–Volterra prey-predator model involving both nonlinear feedback and action threshold depending on the density of pest and its change rate. In the model, we use the action threshold instead of the economic threshold to characterize the implementation of control measures, that is, when the number of pests reaches the action threshold depending on the density of pest and its change rate, a comprehensive pest control tactic is applied so that the number of pests does not exceed the nonlinear ratio-dependent AT. On the other hand, the use of nonlinear controlling factors in the feedback control makes the model closer to reality. Properties of the nonlinear ratio-dependent AT are given. Then, the classification is performed according to the positional relationship between the action threshold level and the stable equilibrium point of the corresponding ordinary differential system. By using the definition and properties of Lambert W function, the analytical expression of the Poincaré map is given. Furthermore, by using the analytical properties of Poincaré map, the existence, uniqueness, and stability of the pest-free and interior-order one periodic solution of the pest-natural enemy system are given, and corresponding sufficient conditions are obtained. The main results are confirmed by numerical simulations.

2. Model Construction and Main Properties of Action Threshold

2.1. Construction of Model. In view of the above objective factors, we propose the following nonlinear state-dependent feedback control model combined with nonlinear ratio-dependent AT:

$$\begin{cases} \left.\begin{aligned} \frac{dx(t)}{dt} &= ax(t) - bx(t)y(t), \\ \frac{dy(t)}{dt} &= cx(t)y(t) - dy(t), \end{aligned}\right\} \theta_1 x(t) + \theta_2 \frac{dx(t)}{dt} < AT, \\ \left.\begin{aligned} x(t^+) &= \left(1 - \frac{\delta x(t)}{x(t)+\alpha}\right)x(t), \\ y(t^+) &= y(t) + \frac{v}{1+\beta y(t)}, \end{aligned}\right\} \theta_1 x(t) + \theta_2 \frac{dx(t)}{dt} = AT. \end{cases} \tag{1}$$

It can be seen that without pulse control measures, the model is simply based on the classical Lotka–Volterra type problem which is extensively used to describe the relation between the populations of pest and natural enemy shown by $x(t)$ and $y(t)$, respectively. Weighted parameters θ_1, θ_2, and AT are positive constants, which satisfy $\theta_1 + \theta_2 = 1$. The discontinuous mapping shown in the third and fourth equations in system (1) represents that the implementation of comprehensive control measures depends on the action level, that is, once the pest density reaches action threshold, the densities of pests as well as the natural enemies are immediately updated to $(1 - \delta x(t)/x(t) + \alpha)x(t)$ and $y(t) + v/1 + \beta y(t)$, respectively. $\alpha > 0$ represents the semisaturation constant, $\delta > 0$ is defined as the maximum instantaneous killing rate after the use of pesticides, and $v > 0$ is the maximum natural enemy when executing the control strategy. The amount $\beta > 0$ is the natural enemy density adjustment parameter. The nonlinear term $v/1 + \beta y(t)$ shows a function of $y(t)$ which decreases monotonically, and the maximum amount of natural enemy release does not exceed. The symbols $x(0^+)$ with $y(0^+)$, respectively, represent the initial populations of pests and natural enemies and satisfy $x(0^+) + y(0^+) < AT$. In model (1), there always exist a stable centre $E_0 = (d/c, a/b)$ and a saddle point $(0, 0)$ which is unstable.

The special cases of the above model for different parameters were considered in [37–39]. The biological significance and main properties of the corresponding ODE model can be seen in [37]. In [38], Tian et al. extended the classic pest-natural enemy model with linear state-dependent control measures to a model with nonlinear state-dependent impulsive control tactics. In [39], the authors for the first time introduced and provided the concept of action threshold depending on the density of pest and its rate of change. They used the definition and properties of the Lambert W function to construct the analytical expression of the Poincaré map. Furthermore, by using the analytical properties of Poincaré map, the existence, uniqueness, and stability of the natural enemy free periodic solution and internal periodic solution were discussed in detail. The results explain the significance of nonlinear ratio-dependent AT in integrated pest control and the important guiding role in IPM strategy.

2.2. Properties of Action Threshold. The quantities θ_1 and θ_2 are dependent weighted parameters. If $\theta_2 = 0$, then the ratio-dependent AT converts into ET. Therefore, we can say that ET is a special case of ratio-dependent AT for $\theta_2 = 0$. Combining the first equation of ODE model (1) with ratio-dependent AT, we get

$$\lim_{x \longrightarrow +\infty} \frac{(\theta_1 + a\theta_2)x - AT}{b\theta_2 x} = \frac{\theta_1 + a\theta_2}{b\theta_2}. \tag{2}$$

If we put $\theta_1 = 0$, then the ratio-dependent AT converts into $y = ax - AT/bx$. In this case, if $x \longrightarrow +\infty$, then y is bounded and reaches its highest value a/b. Further, with the utilization of the control actions on $y = (\theta_1 + a\theta_2)x - AT/b\theta_2 x$, we get another curve $y^+ = (\theta_1 + a\theta_2)x^+ - AT(1 - \delta x(t)/x(t) + \alpha)/b\theta_2 x^+ + v/1 + \beta y$. For $\theta_2 = 0$, the curve changes into $x^+ = (1 - \delta x/x + \alpha)AT$ showing a vertical straight line. Let $P_{AT} = \delta x/x + \alpha$; then, for convenience, we denote the two curves $y = (\theta_1 + a\theta_2)x - AT/b\theta_2 x$ and $y^+ = (\theta_1 + a\theta_2)x^+ - AT(1 - P_{AT})/b\theta_2 x^+ + v/1 + \beta y$ by Γ_{IS} and Γ_{PS}, respectively, as shown in Figure 1.

3. Impulsive and Phase Sets

This section is devoted to present the dynamical aspects of the system (1), and we can use the Poincaré map on the sequence of pulse points which will be formulated later. Let AT/θ_1 be the abscissa of the curves Γ_{IS} at $y = a/b$.

Then, we take the following cases based on the equilibrium E_0 and curve Γ_{IS}.

$$(A)\ \frac{AT}{\theta_1} \leq \frac{d}{c};\ (B)\ \frac{d}{c} < \frac{AT}{\theta_1}. \tag{3}$$

The necessary and primary component is to examine the section that is not used during the pulse effect process, which means that the trajectory initiating from Γ_{PS} cannot touch the curve Γ_{IS} in the case of maximum impulsive set. In the following part of the paper, we address the definition of impulsive sets.

3.1. Impulsive Set. In Case (A), the solution Γ_1 is tangent to the curve Γ_{PS} at point $T = (x_T, y_T)$. If we denote the impulsive set by $\mathscr{M}_1$, then it can be written as

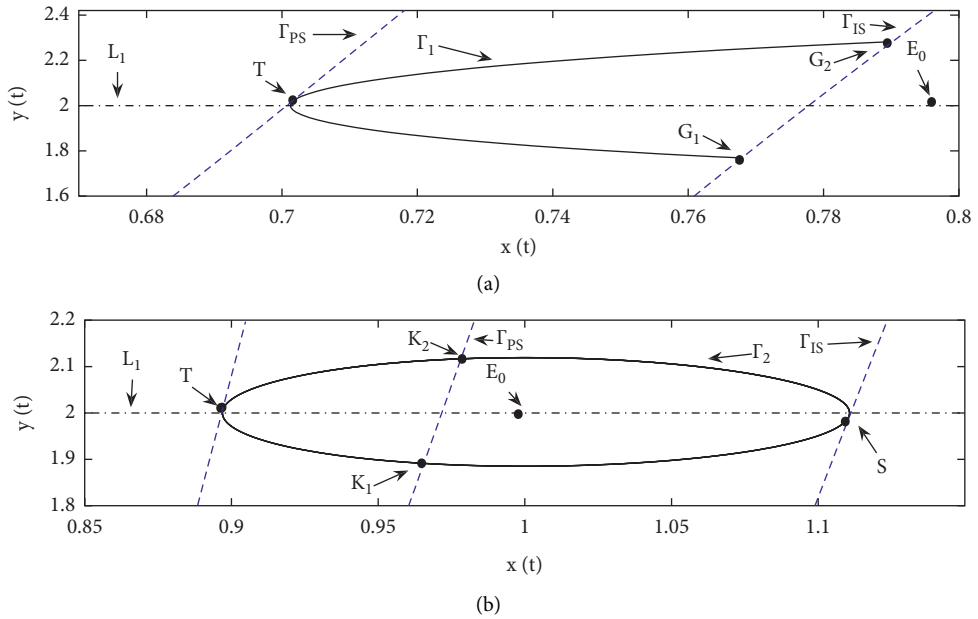

FIGURE 1: Detailed diagrams describing the impulsive along with phase sets where (a) $AT/\theta_1 \le d/c$ and $AT/\theta_1 > d/c$. In sub-plot (a), Γ_1 shows the tangent trajectory to the curve Γ_{PS} and touches the curve Γ_{IS} at (x_{G_2}, y_{G_2}). In sub-plot (b), Γ_2 touches the curve Γ_{PS} at two points (x_{K_1}, y_{K_1}) and (x_{K_2}, y_{K_2}), and tangent to the curve Γ_{IS} at point (x_S, y_S).

$$\mathcal{M}_1 = \left\{(x,y) \in \mathbb{R}^2_+ \middle| \frac{AT}{\theta_1 + a\theta_2} \le x \le x_{G_2}, 0 \le y \le y_{G_2}\right\}. \quad (4)$$

Now based on the corresponding horizontal coordinate, we search the exact value of y_{G_2} in the following lemma. The point y_{G_2} is actually the maximum value of the impulsive set $\mathcal{M}_1$ for Case (A).

Lemma 1. *For Case (A), the maximum impulsive set is defined as $\mathcal{M}_1$ with*

$$y_{G_2} = -\frac{a}{b} W\left(-\frac{b}{a} y_T e^{-b/a y_T + A_{G_2}/a}\right) \text{provided that } A^1_{G_2} \le 0. \quad (5)$$

Proof. Let Γ_1 be a trajectory tangent at $T = (x_T, y_T)$, and it touches the curve Γ_{IS} at point $G_2 = (x_{G_2}, y_{G_2})$. Then, T and G_2 must satisfy the following equation:

$$a \ln y_{G_2} - b y_{G_2} + d \ln x_{G_2} - c x_{G_2} = a \ln y_T - b y_T + d \ln x_T - c x_T. \quad (6)$$

Solving this equation for y_{G_2}, we get

$$\left(-\frac{b}{a} y_{G_2}\right) e^{-b/a y_{G_2}} = -\frac{b}{a} y_T e^{-b/a y_T + A_{G_2}/a}, \quad (7)$$

where $A_{G_2} = d(\ln x_T - \ln x_{Q_2}) + c(x_{G_2} - x_T)$. The above equation obviously gives two solutions when we solve it by using Lambert W function. The minimum solution can be written as follows:

$$y_{G_2} = -\frac{a}{b} W\left(-\frac{b}{a} y_T e^{-b/a y_T + A_{G_2}/a}\right), \quad (8)$$

which is well defined because $A_{G_2} \le 0$.

For Case (B), it is clear from Figure 1(b) that at point $S = (x_S, y_S)$, Γ_2 is tangent to the curve Γ_{IS} where $y_S \le a/b$. Then, taking into account the locations of equilibrium E_0 and the curve Γ_{IS}, we can write the maximum impulsive set for Case (B) as

$$\mathcal{M}_2 = \left\{(x,y) \in \mathbb{R}^2 \middle| \frac{AT}{\theta_1 + a\theta_2} \le x \le x_S, 0 \le y \le y_S\right\}. \quad (9)$$

The above information shows that for this case, the tangent point with Γ_{IS} varies due to small changes in θ_1 and θ_2.

If the weighted parameter θ_2 decreases, then the quantity y_S approaches its maximum value a/b. □

3.2. Phase Set. To determine the exact phase set of system (1) under different conditions, we need to know whether the solution from initial point (x_0^+, y_0^+) reaches the corresponding impulsive set and whether the pulse action occurs or not. To provide the exact domain of phase sets, we first discuss the interval which is free of impulsive effect.

Lemma 2. *For Case (B), any solution starting from the phase set with initial point (x_0^+, y_0^+) (where $y_0^+ \in (y_{K_2}, y_{K_1})$) will not reach the impulsive set $\mathcal{M}_2$, where*

$$y_{K_1} = -\frac{a}{b}W\left(-1, -\frac{b}{a}y_S e^{-b/ay_S - A_{K_1}/a}\right) \text{and } y_{K_2} = -\frac{a}{b}W\left(-\frac{b}{a}y_S e^{-b/ay_S - A_{K_2}/a}\right), \tag{10}$$

provided that $A_{K_1}, A_{K_2} \geq 0$.

Proof. Assume that the closed trajectory Γ_1 starts from $K_1 = (x_{K_1}, y_{K_1})$ and touches the curve Γ_{IS} at point $S = (x_S, y_S)$. Then, K_1 and S must satisfy the following relationship:

$$\begin{aligned} a\ln y_{K_1} - by_{K_1} + d\ln x_{K_1} - cx_{K_1} &= a\ln y_S - by_S \\ &+ d\ln x_S - cx_S. \end{aligned} \tag{11}$$

Rearranging this equation for y_{K_1}, we get

$$\left(-\frac{b}{a}y_{K_1}\right)e^{-b/ay_{K_1}} = -\frac{b}{a}y_S e^{-b/ay_S - A_{K_1}/a}, \tag{12}$$

where $A_{K_1} = d(\ln x_{K_1} - \ln x_S) + c(x_S - x_{K_1})$. The above equation can be easily solved utilizing the Lambert W function approach which clearly will result in two solutions of the problem. The maximum solution can be written as

$$y_{K_1} = -\frac{a}{b}W\left(-1, -\frac{b}{a}y_S e^{-b/ay_S - A_{K_1}/a}\right). \tag{13}$$

The value of y_{K_2} can be found in the similar way as above, i.e.,

$$y_{K_2} = -\frac{a}{b}W\left(-\frac{b}{a}y_S e^{-b/ay_S - A_{K_2}/a}\right), \tag{14}$$

with $A_{K_2} = d(\ln x_{K_2} - \ln x_S) + c(x_S - x_{K_2})$.

As a result, any solution curve initiating from (x_0^+, y_0^+) with $y_0^+ \in (y_{K_2}, y_{K_1})$ will be free from the effect of impulsive set.

For the case when $\theta_2 = 0$, the trajectory shown by Γ_2 becomes tangent at $y = a/b$. So, y_{K_2} and y_{K_1} become

$$y_{K_2} = -\frac{a}{b}W\left(-1, -e^{-1-A_{K_1}/a}\right), \text{and } y_{K_1} = -\frac{a}{b}W\left(-e^{-1-A_{K_2}/a}\right). \tag{15}$$

The impulsive function described by $y(t^+) = y(t) + v/1 + \beta y(t)$ satisfies some properties which are very important.

To do this, we indicate

$$F(u) = u + \frac{v}{1+\beta u}, \quad u \in \left[0, \frac{a}{b}\right], \tag{16}$$

and then we get $F'(u) = 1 - v\beta/(1+\beta u)^2$ and $F'(u) = 0$ at $u = \sqrt{v\beta} - 1/\beta$.

$(A)\mathrm{AT}/\theta_1 \leq d/c$. From Lemma 1, we can describe the impulsive set $\mathcal{M}_1$ as $\mathcal{M}_1 = \{(x, y) \in \mathbb{R}_+^2 | \mathrm{AT}/\theta_1 + a\theta_2 \leq x \leq x_{G_2}, 0 \leq y \leq y_{G_2}\}$. Further, we can take three subclasses as follows.

(i) $\sqrt{v\beta} - 1/\beta \leq 0$.

For this subcase, $F(u) \geq 0$ for all $u \in [0, y_{G_2}]$, which shows that $v \leq F(u) \leq y_{G_2} + v/1 + \beta y_{G_2}$. Then, the corresponding phase set to $\mathcal{M}_1$ can be expressed as

$$\mathcal{N}_{11} = \left\{(x^+, y^+) \in \mathbb{R}_+^2 | x^+ \in X_1^1, y^+ \in Y_1^1\right\}, \tag{17}$$

with

$$\begin{aligned} X_1^1 &= \left[\frac{\mathrm{AT}(1-P_{\mathrm{AT}})}{\theta_1 + a\theta_2}, (1-P_{\mathrm{AT}})x_{G_2}\right], \\ Y_1^1 &= \left[v, y_{G_2} + \frac{v}{1+\beta y_{G_2}}\right]. \end{aligned} \tag{18}$$

(ii) $\sqrt{v\beta} - 1/\beta \geq y_{G_2}$.

For this subcase, $F(u) \leq 0$ for $u \in [0, y_{G_2}]$, which denotes that $y_{G_2} + v/1 + \beta y_{G_2} \leq F(u) \leq v$. Then, the corresponding phase set to $\mathcal{M}_1$ is expressed as follows:

$$\mathcal{N}_{12} = \left\{(x^+, y^+) \in \mathbb{R}_+ \times \mathbb{R}_+ | x^+ \in X_2^1, y^+ \in Y_2^1\right\}, \tag{19}$$

with

$$\begin{aligned} X_2^1 &= \left[(1-P_{\mathrm{AT}})x_{G_2}, \frac{\mathrm{AT}(1-P_{\mathrm{AT}})}{\theta_1 + a\theta_2}\right], \\ Y_2^1 &= \left[y_{G_2} + \frac{v}{1+\beta y_{G_2}}, v\right]. \end{aligned} \tag{20}$$

(iii) $0 < \sqrt{v\beta} - 1/\beta < y_{G_2}$.

For the present subcase, the impulsive set $\mathcal{M}_1$ becomes $\mathcal{M}_1 = \mathcal{M}_{11} \cup \mathcal{M}_{12}$, where

$$\mathcal{M}_{11} = \left\{(x, y) \in \mathbb{R}_+^2 | x \in X_3^1, y \in Y_3^1\right\}, \tag{21}$$

with

$$\begin{aligned} X_3^1 &= \left[\frac{\mathrm{AT}}{\theta_1 + a\theta_2}, \frac{\mathrm{AT}\beta}{(\theta_1 + a\theta_2)\beta - (\sqrt{v\beta} - 1)b\theta_2}\right], \\ Y_3^1 &= \left[0, \frac{\sqrt{v\beta} - 1}{\beta}\right], \end{aligned} \tag{22}$$

$$\mathcal{M}_{12} = \left\{(x, y) \in \mathbb{R}_+^2 | < x \in X_4^1, y \in Y_4^1\right\}, \tag{23}$$

with

$$\begin{aligned} X_4^1 &= \left(\frac{\mathrm{AT}\beta}{(\theta_1 + a\theta_2)\beta - (\sqrt{v\beta} - 1)b\theta_2}, x_{G_2}\right], \\ Y_4^1 &= \left(\frac{\sqrt{v\beta} - 1}{\beta}, y_{G_2}\right]. \end{aligned} \tag{24}$$

Hence, the corresponding phase set to the impulsive set $\mathcal{M}_1 = \mathcal{M}_{11} \cup \mathcal{M}_{12}$ is $\mathcal{N}_{13} \cup \mathcal{N}_{14}$, where

$$\mathcal{N}_{13} = \left\{(x^+, y^+) \in \mathbb{R}_+^2 | x^+ \in X_5^1, y^+ \in Y_5^1\right\}, \tag{25}$$

with

$$X_5^1 = \left[\frac{\mathrm{AT}(1-P_{\mathrm{AT}})\beta}{(\theta_1 + a\theta_2)\beta - (\sqrt{v\beta} - 1)b\theta_2}, \frac{\mathrm{AT}(1-P_{\mathrm{AT}})}{\theta_1 + a\theta_2}\right],$$
$$Y_5^1 = \left[\frac{2\sqrt{v\beta} - 1}{\beta}, v\right], \tag{26}$$

$$\mathcal{N}_{14} = \left\{(x^+, y^+) \in \mathbb{R}_+^2 | x^+ \in X_6^1, y^+ \in Y_6^1\right\}, \tag{27}$$

with

$$X_6^1 = \left(\frac{\mathrm{AT}(1-P_{\mathrm{AT}})\beta}{(\theta_1 + a\theta_2)\beta - (\sqrt{v\beta} - 1)b\theta_2}, (1-P_{\mathrm{AT}})x_{G_2}\right],$$
$$Y_6^1 = \left(\frac{2\sqrt{v\beta} - 1}{\beta}, y_{G_2} + \frac{v}{1+\beta y_{G_2}}\right]. \tag{28}$$

(B) $d/c < \mathrm{AT}/\theta_1$. For this case, we express the impulsive set as follows.

$\mathcal{M}_2 = \{(x, y) \in \mathbb{R}_+ \times \mathbb{R}_+ | \mathrm{AT}/\theta_1 + a\theta_2 \le x \le x_S, 0 \le y \le y_S\}$. In order to give the exact domain of phase sets for Case (B), based on Lemma 2, we describe the following sets:

$$X_D^l = \left[\frac{\mathrm{AT}(1-P_{\mathrm{AT}})}{(\theta_1 + a\theta_2 + vb\theta_2)}, x_{K_2}\right] \cup \left[x_{K_1}, \infty\right),$$
$$Y_D^l = \left[0, y_{K_2}\right] \cup \left[y_{K_1}, \frac{(\theta_1 + a\theta_2)}{b\theta_2} + \frac{b\theta_2 v}{b\theta_2 + \beta(\theta_1 + a\theta_2)}\right). \tag{29}$$

The following three subcases can be taken based on the definition of the phase set.

(i) $\sqrt{v\beta} - 1/\theta \le 0$.

For this subcase, $F(u) \ge 0$ for all values of u belongs to $[0, y_S]$. This shows that $v \le F(u) \le y_S + v/1 + \beta y_S$. The corresponding phase set to $\mathcal{M}_2$ can be expressed as

$$\mathcal{N}_{21} = \left\{(x^+, y^+) \in \mathbb{R}_+ \times \mathbb{R}_+ | x^+ \in X_1^2, y^+ \in Y_1^2\right\}, \tag{30}$$

with

$$X_{21}^0 = \left[\frac{\mathrm{AT}(1-P_{\mathrm{AT}})}{\theta_1 + a\theta_2}, (1-P_{\mathrm{AT}})x_S\right],$$
$$X_1^2 = X_D^l \cap X_{21}^0, \tag{31}$$

$$Y_{21}^0 = \left[v, y_S + \frac{v}{1+\beta y_S}\right],$$
$$Y_1^2 = Y_D^l \cap Y_{21}^0. \tag{32}$$

(ii) $\sqrt{v\beta} - 1/\beta \ge y_S$.

For this subcase, $F(u) \le 0$ for $u \in [0, y_S]$, which denotes that $y_S + v/1 + \beta y_S \le F(u) \le v$. Hence, the phase set corresponding to $\mathcal{M}_2$ is given as

$$\mathcal{N}_{22} = \left\{(x^+, y^+) \in \mathbb{R}_+ \times \mathbb{R}_+ | x^+ \in X_2^2, y^+ \in Y_2^2\right\}, \tag{33}$$

with

$$X_{22}^0 = \left[(1-P_{\mathrm{AT}})x_S, \frac{\mathrm{AT}(1-P_{\mathrm{AT}})}{\theta_1 + a\theta_2}\right],$$
$$X_2^2 = X_D^l \cap X_{22}^0, \tag{34}$$

$$Y_{22}^0 = \left[y_S + \frac{v}{1+\beta y_S}, v\right],$$
$$Y_2^2 = Y_D^l \cap Y_{22}^0. \tag{35}$$

(iii) $0 < \sqrt{v\beta} - 1/\beta < y_S$.

If $0 \le u \le \sqrt{v\beta} - 1/\beta$, then $F(u) \le 0$ and $2\sqrt{v\beta} - 1/\beta \le F(u) \le v$. If $\sqrt{v\theta} - 1/\beta < u \le y_S$, then $F(u) > 0$ and $2\sqrt{v\beta} - 1/\beta < F(u) \le y_S + v/1 + \beta y_S$.

The impulsive set $\mathcal{M}_2$ is now can be explained in the form $\mathcal{M}_2 = \mathcal{M}_{21} \cup \mathcal{M}_{22}$, where

$$\mathcal{M}_{21} = \left\{(x, y) \in \mathbb{R}_+^2 | x \in X_3^2, y \in Y_3^2\right\}, \tag{36}$$

with

$$X_3^2 = \left[\frac{\mathrm{AT}}{\theta_1 + a\theta_2}, \frac{\mathrm{AT}\beta}{(\theta_1 + a\theta_2)\beta - (\sqrt{v\beta} - 1)b\theta_2}\right],$$
$$Y_3^2 = \left[0, \frac{\sqrt{v\beta} - 1}{\beta}\right], \tag{37}$$

and

$$\mathcal{M}_{22} = \left\{(x, y) \in \mathbb{R}_+^2 | x \in X_4^2, y \in Y_4^2\right\}, \tag{38}$$

with

$$X_4^2 = \left(\frac{\mathrm{AT}\beta}{(\theta_1 + a\theta_2)\beta - (\sqrt{v\beta} - 1)b\theta_2}, x_S\right],$$
$$Y_4^2 = \left(\frac{\sqrt{v\beta} - 1}{\beta}, y_S\right]. \tag{39}$$

Hence, the phase set corresponding to the impulsive set $\mathcal{M}_2 = \mathcal{M}_{21} \cup \mathcal{M}_{22}$ can be expressed as $\mathcal{N}_{23} \cup \mathcal{N}_{24}$, where

$$\mathcal{N}_{23} = \left\{(x^+, y^+) \in \mathbb{R}_+^2 | x^+ \in X_5^2, y^+ \in Y_5^2\right\}, \tag{40}$$

with

$$X_{23}^{0}=\left(\frac{\mathrm{AT}(1-P_{\mathrm{AT}})\beta}{(\theta_1+a\theta_2)\beta-(\sqrt{v\beta}-1)b\theta_2},\frac{\mathrm{AT}(1-P_{\mathrm{AT}})}{\theta_1+a\theta_2}\right],\ X_5^2=X_D^l\cap X_{23}^0,$$
$$Y_{23}^{0}=\left[\frac{2\sqrt{v\beta}-1}{\beta},v\right],\ Y_5^2=Y_D^l\cap Y_{23}^0, \tag{41}$$

$$\mathcal{N}_{24}=\left\{(x^+,y^+)\in\mathbb{R}_+^2|x^+\in X_6^2,y^+\in Y_6^2\right\}, \tag{42}$$

with

$$X_{24}^{0}=\left(\frac{\mathrm{AT}(1-P_{\mathrm{AT}})\beta}{(\theta_1+a\theta_2)\beta-(\sqrt{v\beta}-1)b\theta_2},(1-P_{\mathrm{AT}})x_S\right],$$
$$X_6^2=X_D^l\cap X_{24}^0, \tag{43}$$

$$Y_{24}^{0}=\left(\frac{2\sqrt{v\beta}-1}{\beta},y_S+\frac{v}{1+\beta y_S}\right],$$
$$Y_6^2=Y_D^l\cap Y_{24}^0. \tag{44}$$

For Case (A), if $\mathrm{AT}/\theta_1\le d/c$, then the solution from the phase set does not reach the interval $(y_{G_2},a/b]$. It is also important to note that if $y_T=a/b$ and $A_{G_2}=0$, then $y_{G_2}=a/b$. For Case (B), it can be seen from the vector field of system (1) that if the closed orbit is tangent or does not touch the curve Γ_{PS}, then there must be a trajectory that is tangent to the curve Γ_{PS} at a point (x_T,y_T), and the trajectory intersects the curve Γ_{IS} at lower point G_2. This proves that the impulsive set in this case is defined by $\mathscr{M}_1$, as shown in Figure 1(b).

If the closed trajectory is tangent to Γ_{IS} at point $S=(x_S,y_S)$ and intersects the curve Γ_{PS} at two points, then it can be seen that for any solution from the phase set, it is impossible to reach the interval $(y_S,a/b]$. The above theory shows that nonlinear terms of the controlling measure combined with nonlinear action threshold make impulse system (1) quite complicated, and it is very difficult to analyze each situation in detail. □

4. Poincaré Map

Poincaré map [40–42] plays a very helpful role in examining the qualitative behavior of a dynamical system, most prominently the asymptotic stability of periodic or almost periodic orbits. Based on the impulse and phase sets discussed above, the following related theorem for Poincaré map can be obtained.

Theorem 1. *For the impulsive points of model (1), the Poincaré map for Cases* $(A)$and(B) *has the following form.*

(A) $AT/\theta_1\le d/c$*:*

$$y_{i+1}^{+}=\begin{cases}\psi(y_i^+),y_i^+\in Y_1^1,\text{if }\dfrac{\sqrt{v\beta}-1}{\beta}\le 0,\\ \psi(y_i^+),y_i^+\in Y_2^1,\text{if }\dfrac{\sqrt{v\beta}-1}{\beta}\ge y_{G_2},\\ \psi(y_i^+),y_i^+\in Y_5^1\cup Y_6^1,\text{if }0<\dfrac{\sqrt{v\beta}-1}{\beta}<y_{G_2}.\end{cases} \tag{45}$$

(B) $d/c<AT/\theta_1$*:*

$$y_{i+1}^{+}=\begin{cases}\psi(y_i^+),y_i^+\in Y_1^2,\text{if }\dfrac{\sqrt{v\beta}-1}{\beta}\le 0,\\ \psi(y_i^+),y_i^+\in Y_2^2,\text{if }\dfrac{\sqrt{v\beta}-1}{\beta}\ge y_S,\\ \psi(y_i^+),y_i^+\in Y_5^2\cup Y_6^2,\text{if }0<\dfrac{\sqrt{v\beta}-1}{\beta}<y_S,\end{cases} \tag{46}$$

where

$$\psi(y_i^+)=-\frac{a}{b}W\left[-\frac{b}{a}y_i^+\exp\left(-\frac{b}{a}y_i^++\frac{A_l}{a}\right)\right]+\frac{v}{1-\beta a/bW\left[-b/ay_i^+\exp\left(-b/ay_i^++A_l/a\right)\right]}. \tag{47}$$

Proof. Suppose that a trajectory initiating from (x_0^+,y_0^+) repeats k (finite or infinite) times pulse action. Let the points of the impulse set be represented by $p_i=(x_i,y_i)$, and after the pulse action, the corresponding points of phase set are represented by $p_i^+=(x_i^+,y_i^+)$. If $p_0^+=(x_i^+,y_i^+)\in\Gamma_{\mathrm{PS}}$ and $p_1=(x_{i+1},y_{i+1})\in\Gamma_{\mathrm{IS}}$ are on the same trajectory above, then the coordinates of the two points satisfy the following trajectory equation:

$$d\ln x_i^+ - d\ln x_{i+1} + \mathrm{cx}_{i+1} - \mathrm{cx}_i^+ = a\ln\frac{y_{i+1}}{y_i^+} - b\left(y_{i+1} - y_i^+\right). \tag{48}$$

Solving the above equation for y_{i+1}, we get

$$y_{i+1} = -\left(\frac{a}{b}\right)W\left[-\frac{b}{a}y_i^+\exp\left(-\frac{b}{a}y_i^+ + \frac{A_1}{a}\right)\right], \tag{49}$$

where

$$A_l = d\ln x_i^+ - d\ln x_{i+1} + \mathrm{cx}_{i+1} - \mathrm{cx}_i^+, \tag{50}$$

and therefore

$$\psi\left(y_i^+\right) = -\frac{a}{b}W\left[-\frac{b}{a}y_i^+\exp\left(-\frac{b}{a}y_i^+ + \frac{A_1}{a}\right)\right] + \upsilon/1 - \frac{\beta a}{b}W\left[-\frac{b}{a}y_i^+\exp\left(-\frac{b}{a}y_i^+ + \frac{A_l}{a}\right)\right] = y_{i+1}^+. \tag{51}$$

From above equation, we can see that the Poincaré map given in (47) depends on both the Lambert W function and the sign of A_l.

Case. (A). If $A_l \le 0$, then for $y_i^+ \ge 0$, the above expressions defined in (9) and (10) are well defined. Further, if we define $g(y) = -b/ay\exp(-b/ay)$, then it is easy to prove that $g(y)$ achieved its minimum value $-e^{-1}$ at $y = a/b$. Therefore, $-b/ay\exp(-b/ay)\exp(A_l/a) \in [-e^{-1}, 0)$ for all $A_l \le 0$ and $y > 0$. This denotes that the Poincaré map defined relative to Case (A) is (7).

Table 1: The exact impulsive and phase sets for system (1) under Cases (A) and (B).

Cases		Condition	Impulsive set	Phase set
(A)	(i)	$\frac{\mathrm{AT}}{\theta_1} \le \frac{d}{c}$	$\mathscr{M}_1$	$\mathscr{N}_{11}$
	(ii)			$\mathscr{N}_{12}$
	(iii)			$\mathscr{N}_{13} \cup \mathscr{N}_{14}$
(B)	(i)	$\frac{\mathrm{AT}}{\theta_1} \le \frac{d}{c}$	$\mathscr{M}_2$	$\mathscr{N}_{21}$
	(ii)			$\mathscr{N}_{22}$
	(iii)			$\mathscr{N}_{23} \cup \mathscr{N}_{24}$

For Case (B), if $A_l > 0$, then $-b/ay\exp(-b/ay)\exp(A_l/a) \ge -\exp(-1)$. From this, we obtain the following:

$$\left(\frac{b}{a}\right)y\exp\left(-y\frac{b}{a}\right) \le \exp\left(-\left[1 + \frac{A_l}{a}\right]\right). \tag{52}$$

This solution further simplifies as $y \in (0, y_{K_2}] \cup [y_{K_1}, (\theta_1 + a\theta_2)/b\theta_2 + b\theta_2\upsilon/b\theta_2 + \beta(\theta_1 + a\theta_2))$, and from Lemma 2 we know that

$$y_{K_2} = -\frac{a}{b}W\left(-\frac{b}{a}y_S e^{-b/ay_S - A_{K_2}/a}\right) \text{ and } y_{K_1} = -\frac{a}{b}W\left(-1, -\frac{b}{a}y_S e^{-b/ay_S - A_{K_1}/a}\right). \tag{53}$$

Hence, in the same way, the Poincaré map domain for all remaining cases provided in Section 3 and Table 1 can be found. This finalized the proof. □

5. Characteristics of Poincaré Map

To discuss the existence as well as the stability for the order-1 periodic solution of problem (1), we first analyze the different characteristics of Poincaré map for the above existing cases. For this, we define an important point $G = (x_G, y_G) = (\mathrm{AT}\beta/(\theta_1 + a\theta_2)\beta - (\sqrt{\upsilon\beta} - 1)b\theta_2, \sqrt{\upsilon\beta} - 1/\beta)$ which will be used in the following discussion. If $G \in \Gamma_{\mathrm{IS}}$, then after one time pulse, the corresponding impulse point can be presented as G^+: $(x_{G^+}, y_{G^+}) = (\mathrm{AT}(1 - P_{\mathrm{AT}})\ \beta/(\theta_1 + a\theta_2)\beta - (\sqrt{\upsilon\beta} - 1)b\theta_2, 2\sqrt{\upsilon\beta} - 1/\beta)$.

Theorem 2. *The Poincaré map $\psi(y_i^+)$ for Cases (A) and (B) provided in Table 2 satisfies different properties as follows:*

(A) $AT/\theta_1 \le d/c$ and $A_l \le 0$.

(i) It shows increasing behavior on $[0, y_T]$ and decreasing behavior on $[y_T, \theta_1 + a\theta_2/b\theta_2 + b\theta_2\upsilon/b\theta_2 + \beta(\theta_1 + a\theta_2))$ for $\sqrt{\upsilon\beta} - 1/\beta \le 0$.

(ii) It is increasing on $[y_T, \theta_1 + a\theta_2/b\theta_2 + b\theta_2\upsilon/b\theta_2 + \beta(\theta_1 + a\theta_2))$ and decreasing on $[0, y_T]$ for $\sqrt{\upsilon\beta} - 1/\beta \ge y_{G_2}$.

(iii) It is decreasing on $[0, y_{n_2}]$ and $[y_T, y_{n_1}]$ and increasing on $[y_{n_2}, y_T]$ and $[y_{n_1}, \theta_1 + a\theta_2/b\theta_2 + b\theta_2\upsilon/b\theta_2 + \beta(\theta_1 + a\theta_2))$ for $0 < \sqrt{\upsilon\beta} - 1/\beta < y_{G_2}$, where $y_{n_2} = \min\{y^+ : \psi(y^+) = y_{G^+}\}$, $y_{n_1} = \max\{y^+ : \psi(y^+) = y_{G^+}\}$.

(B) $d/c < AT/\theta_1$ and $A_l > 0$.

(i) It shows increasing behavior over the closed interval $[0, y_{K_2}]$ and decreasing behavior on $[y_{K_1}, \theta_1 + a\theta_2/b\theta + b\theta_2\upsilon/b\theta_2 + \beta(\theta_1 + a\theta_2)$ for $\sqrt{\upsilon\beta} - 1/\beta \le 0$.

(ii) It is increasing on $[y_{K_1}, \theta_1 + a\theta_2/b\theta_2 + b\theta_2\upsilon/b\theta_2 + \beta(\theta_1 + a\theta_2))$ and decreasing on $[0, y_{K_2}]$ for $\sqrt{\upsilon\beta} - 1/\beta \ge y_S$.

Table 2: The domain of the Poincaré map for Cases (A) and (B).

Cases		Condition	A_l	$\psi(y_i^+)$
(A)	(i)	$\mathrm{AT}/\theta_1 \le d/c$	$A_l \le 0$	$y_i^+ \in Y_1^1$
	(ii)			$y_i^+ \in Y_2^1$
	(iii)			$y_i^+ \in Y_5^1 \cup Y_6^1$
(B)	(i)	$\mathrm{AT}/\theta_1 \le d/c$	$A_l > 0$	$y_i^+ \in Y_1^2$
	(ii)			$y_i^+ \in Y_2^2$
	(iii)			$y_i^+ \in Y_5^2 \cup Y_6^2$

(iii) It is decreasing on $[0, y_{N_2}]$ *and* $[y_{K_1}, y_{N_1}]$ *and increasing on* $[y_{N_2}, y_{K_2}]$ *and* $[y_{N_1}, \theta_1 + a\theta_2/b\theta_2 + b\theta_2 v/b\theta_2 + \beta(\theta_1 + a\theta_2))$ *for* $0 < \sqrt{v\beta} - 1/\beta < y_S$, *where* $y_{N_2} = \min\{y^+ : \psi(y^+) = y_{G^+}\}$, $y_{N_1} = \max\{y^+ : \psi(y^+) = y_{G^+}\}$.

Proof. Assuming that $q_i^+ = (x_i^+, y_i^+) \in \Gamma_{PS}$, the solution initiating from q_i^+ intersects the curve Γ_{IS} at $q_{i+1} = (x_{i+1}, y_{i+1})$. If q_i^+ and q_{i+1} lie in one trajectory, then y_{i+1} is established by y_i^+ and can be expressed as $y_{i+1} = F(y_i^+)$. The corresponding vector field relative of the system given in (1) confirms that the domain of consideration of Poincaré map $\psi(y_i^+)$ for Case $(A)(i)$ is defined by $[0, y_T] \cup [y_T, \theta_1 + a\theta_2/b\theta_2 + b\theta_2 v/b\theta_2 + \beta(\theta_1 + a\theta_2))$. Furthermore, for this case, the corresponding impulsive function F has increasing behavior over the closed interval $[0, y_T]$. Therefore, based on the definition of $\psi(y_i^+)$, it is increasing on $[0, y_T]$ and decreasing on $[y_T, \theta_1 + a\theta_2/b\theta_2 + b\theta_2 v/b\theta_2 + \beta(\theta_1 + a\theta_2))$. The function F is decreasing upon $[0, y_T]$ in Case $(A)(ii)$, which shows that $\psi(y_i^+)$ is decreasing over the interval $[0, y_T]$ and increasing over the closed interval $[y_T, \theta_1 + a\theta_2/b\theta_2 + b\theta_2 v/b\theta_2 + \beta(\theta_1 + a\theta_2))$. For Case $(A)(iii)$, F is decreasing over $[0, y_G]$ and increasing upon $[y_G, y_T]$. Therefore, $\psi(y_i^+)$ is decreasing on $[0, y_{N_2}]$ and $[y_{K_1}, y_{N_1}]$ and increasing on $[y_{N_2}, y_{K_2}]$ and $[y_{N_1}, \theta_1 + a\theta_2/b\theta_2 + b\theta_2 v/b\theta_2 + \beta(\theta_1 + a\theta_2))$.

By using the same methods as above, we can prove that the monotonicities of the Poincaré map for Cases $(B)(i)$, (ii), (iii) in Theorem 2 are true. □

Lemma 3. *If* $A_l > 0$ *and* $v > 0$, *then the inequality*

$$\psi(y_i^+) > y_i^+, \text{for all } y_i^+ \in \left(0, y_{K_2}\right), \tag{54}$$

is fulfilled for the corresponding Poincaré map shown by $\psi(y_i^+)$.

Proof. Let a solution originate from $p_0^+ = (x_i^+, y_i^+)$, and it touches the curve Γ_{IS} at point $p_1 = (x_{i+1}, y_{i+1})$. We assume that $y_i^+, y_{i+1} < a/b$; then,

$$\begin{aligned} a \ln y_{i+1} - \mathrm{by}_{i+1} + d \ln x_{i+1} - \mathrm{cx}_{i+1} &= a \ln y_i^+ - \mathrm{by}_i^+ \\ &\quad + d \ln x_i^+ - \mathrm{cx}_i^+. \end{aligned} \tag{55}$$

From (55), we get

$$-\frac{b}{a} y_{i+1} e^{(-b/a y_{i+1})} = -\frac{b}{a} y_i^+ e^{(-b/a y_i^+ + A_l/a)}. \tag{56}$$

If $A_l > 0$, then we get the inequality

$$-\frac{b}{a} y_{i+1} e^{(-b/a y_{i+1})} < -\frac{b}{a} y_i^+ e^{(-b/a y_i^+)}. \tag{57}$$

Let $f(y) = -y \exp(-y)$; then, $f'(y) > 0$ if $y > 1$ and $f'(y) < 0$ if $y \in (0, 1)$. The inequality $y_{i+1} > y_i^+$ is satisfied for all $b/a y_i^+, b/a y_{i+1} \in (0, 1)$. We also know that $y_{i+1}^+ = y_{i+1} + v$ and $\psi(y_i^+) = y_{i+1}^+$. Hence, we deduce that $\psi(y_i^+) > y_i^+$ for all $y_i^+ \in (0, y_{K_2})$.

In light of the above explained properties of Poincaré map, the existence of the fixed point of Poincaré map $\psi(y_i^+)$ for $v > 0$ is discussed in following section. □

6. Characteristics of Boundary Periodic Solution

In Section 4, the formula for Poincaré map $\psi(y_i^+)$ has been attained. We will use this formula to study the existence of fixed point, where the fixed point is indicated as y^*, satisfying $\psi(y^*) = y^*$, such as

$$y^* = -\frac{a}{b} W \times \left[\left(-\frac{b}{a}\right) y^* \exp\left(-\frac{b}{a} y^* + \frac{A_l}{a}\right)\right] + \frac{v}{1 - \beta a/bW\left[-b/a y^* \exp\left(-b/a y^* + A_l/a\right)\right]}. \tag{58}$$

For $v = 0$, we get the following equation from above:

$$y^* = -\left(\frac{a}{b}\right) W\left[-\frac{b}{a} y^* \exp\left(-\frac{b}{a} y^* + \frac{A_l}{a}\right)\right]. \tag{59}$$

If $A_l = 0$, the fixed point shown by y^* of the respective Poincaré map $\psi(y_i^+)$ becomes

$$y^* = -\left(\frac{a}{b}\right) W\left[-\frac{b}{a} y^* \exp\left(-\frac{b}{a} y^*\right)\right]. \tag{60}$$

This shows that if $v = 0$, $A_l = 0$, then every point is the fixed point of $\psi(y_i^+)$. If $v = 0$, $A_l \neq 0$, then y^* (a fix point) of the $\psi(y_i^+)$ fulfils

$$y^* = -\left(\frac{a}{b}\right) W\left[-\frac{b}{a} y^* \exp\left(-\frac{b}{a} y^* + \frac{A_l}{a}\right)\right]. \tag{61}$$

In this case, $\psi(y^*) = y^*$ holds $\Leftrightarrow y^* = 0$. Thus, we deduced that $y^* = 0$ is a unique fixed point for system (1).

In the following result, we present the conditions of global stability for boundary order-1 periodic solution. To demonstrate it, we first discuss an important lemma [43, 44].

Lemma 4. *The T-periodic solution* $(x, y) = (\zeta(t), \xi(t))$ *of system*

$$\begin{cases} \dfrac{\mathrm{d}x}{\mathrm{d}t} = C(x, y), \dfrac{\mathrm{d}y}{\mathrm{d}t} = D(x, y), \text{if } \theta(x, y) \neq 0, \\ x^{+} = x + \varepsilon(x, y), y^{+} = y + \varepsilon(x, y), \text{if } \theta(x, y) = 0, \end{cases} \tag{62}$$

is orbitally asymptotically stable if the Floquet multiplier μ_2 *satisfies* $|\mu_2| < 1$, *where*

$$\mu_2 = \prod_{j=1}^{k} \Delta_j \exp\left(\int_0^T \left[\frac{\partial C}{\partial x}(\zeta(t), \xi(t)) + \frac{\partial D}{\partial y}(\zeta(t), \xi(t)) \right] \mathrm{d}t \right), \tag{63}$$

with

$$\Delta_j = \frac{C_+ (\partial\varepsilon/\partial y \partial\theta/\partial x - \partial\varepsilon/\partial x \partial\theta/\partial y + \partial\theta/\partial x) + D_+ (\partial\epsilon/\partial x \partial\theta/\partial y - \partial\epsilon/\partial y \partial\theta/\partial x + \partial\theta/\partial y)}{C\partial\theta/\partial x + B\partial\theta/\partial y}, \tag{64}$$

and θ *is continuously differentiable corresponding to both* x, y. $C, D, \partial\epsilon/\partial x, \partial\epsilon/\partial y, \partial\varepsilon/\partial x, \partial\varepsilon/\partial y, \partial\theta/\partial x$ *and* $\partial\theta/\partial y$ *are evaluated at* $(\zeta(t_j), \xi(t_j))$, $C_+ = C(\zeta(t_j^+), \xi(t_j^+))$ *and* $D_+ = D(\zeta(t_j^+), \xi(t_j^+))$, *and* t_j $(j, k \in \mathbb{N}$, $\mathbb{N}$ *is the set of non-negative integers) is the time of the j-th jump.*

Theorem 3. *If* $A_l = 0$ *and* $v = 0$, *then the fixed point* y^* *of Poincaré map* $\psi(y_i^+)$ *is stable in the phase set. If* $A_l < 0$ *and* $v = 0$, *then* $(x^T(t), 0)$ *is globally asymptotically stable. If* $A_l > 0$ *and* $v = 0$, *then it is unstable.*

Proof. If $v = 0$, $A_l = 0$, then y^* in the phase set is a fixed point of the Poincaré map $\psi(y_i^+)$. This case confirms the stable solution of the problem but is not asymptotically stable. We first show that when $y(t) = 0$ if and only if $v = 0$, and then boundary order-1 periodic solution exists for system (1). For $y(t) = 0$, system (1) is converted into the subsystem given below:

$$\begin{cases} \dfrac{\mathrm{d}x(t)}{\mathrm{d}t} = a \times x(t), \quad x(t) < \dfrac{\mathrm{AT}}{\theta_1 + a\theta_2}, \\ x(t^+) = x(t)\left(1 - \dfrac{\delta x(t)}{x(t) + \alpha}\right), \quad x(t) = \dfrac{\mathrm{AT}}{\theta_1 + a\theta_2}, \end{cases} \tag{65}$$

The first equation of the subsystem (14), combining with the respective initial condition shown as $x(0^+) = (1 - P_{\mathrm{AT}})\mathrm{AT}/\theta_1 + a\theta_2$, where $P_{\mathrm{AT}} = \delta x(t)/x(t) + \alpha$, gives us the solution

$$x(t) = (1 - P_{\mathrm{AT}}) \frac{\mathrm{AT}}{\theta_1 + a\theta_2} \exp(\mathrm{at}). \tag{66}$$

Taking the equation $\mathrm{AT}/\theta_1 + a\theta_2 = (1 - P_{\mathrm{AT}})\mathrm{AT}/\ \theta_1 + a\theta_2 \exp(\mathrm{aT})$ and evaluating it for T, we get $T = -1/a\ln(1 - P_{\mathrm{AT}})$. This shows that T-periodic boundary order-1 solution exists for system (1) as

$$\left(x^T(t), 0\right) = \left((1 - P_{\mathrm{AT}}) \frac{\mathrm{AT}}{\theta_2 + a\theta_2} \exp(\mathrm{at}), 0 \right). \tag{67}$$

Next, we show that $(x^T(t), 0)$ is asymptotically stable. For this, we apply Lemma 4 and present the following.

Method 1.

$$\begin{gathered} C(x, y) = (a - \mathrm{by})x, D(x, y) = y(\mathrm{cx} - d), \\ \varepsilon(x, y) = -P_{\mathrm{AT}} x, \varepsilon(x, y) = \frac{v}{1 + \beta y}, \theta(x, y) = (\theta_1 + a\theta_2)x - b\theta_2 \mathrm{xy} - \mathrm{AT}, \\ \left(x^T(T), y^T(T)\right) = \left(\frac{\mathrm{AT}}{\theta_1 + a\theta_2}, 0 \right), \left(x^T(T^+), y^T(T^+)\right) = \left((1 - P_{\mathrm{AT}}) \frac{\mathrm{AT}}{\theta_1 + a\theta_2}, 0 \right). \end{gathered} \tag{68}$$

From the above, we get

$$\frac{\partial C}{\partial x} = a - \mathrm{by}, \frac{\partial D}{\partial y} = \mathrm{cx} - d, \frac{\partial \varepsilon}{\partial x} = \frac{-\delta x^2 + 2\delta\alpha x}{(x+\alpha)^2}, \frac{\partial \varepsilon}{\partial x} = \frac{\upsilon\beta}{(1+\beta y)^2},$$
$$\frac{\partial \theta}{\partial x} = \theta_1 + a\theta_2 - b\theta_2 y, \frac{\partial \theta}{\partial y} = -b\theta_2 x, \frac{\partial \varepsilon}{\partial y} = \frac{\partial \varepsilon}{\partial y} = 0, \tag{69}$$

$$\begin{aligned}\Delta_1 &= \frac{C_+(\partial\varepsilon/\partial y\partial\theta/\partial x - \partial\varepsilon/\partial x\partial\theta/\partial y + \partial\theta/\partial x) + D_+(\partial\varepsilon/\partial x\partial\theta/\partial y - \partial\varepsilon/\partial y\partial\theta/\partial x + \partial\theta/\partial y)}{C\partial\theta/\partial x + D\partial\theta/\partial y} \\ &= \frac{C^+\left(x^T(T^+), y^T(T^+)\right)(\theta_1 + a\theta_2 - b\theta_2 y) + D^+\left(x^T(T^+), y^T(T^+)\right)(P_{\mathrm{AT}} b\theta_2 x - b\theta_2 x)}{C\left(x^T(T), y^T(T)\right)(\theta_1 + a\theta_2 - b\theta_2 y) - D\left(x^T(T), y^T(T)\right)(b\theta_2 x)} \\ &= (1 - P_{\mathrm{AT}}).\end{aligned} \tag{70}$$

Based on the above information, the Floquet multiplier denoted by μ_2 is defined as

$$\begin{aligned}\mu_2 &= \Delta_1 \exp\left(\int_0^T \left[\frac{\partial C}{\partial x}\left(x^T(t), y^T(t)\right) + \frac{\partial D}{\partial y}\left(x^T(t), y^T(t)\right)\right]\mathrm{d}t\right) \\ &= (1 - P_{\mathrm{AT}})\exp\left(\ln\frac{1}{1 - P_{\mathrm{AT}}} + \frac{A_l}{a}\right) \\ &= \exp\left(\frac{A_l}{a}\right).\end{aligned} \tag{71}$$

If $A_l < 0$ and $\upsilon = 0$, then we get $|\mu_2| < 1$. This indicates that for the problem described in (1), the boundary order-1 periodic solution $(x^T(t), 0)$ is orbitally stable asymptotically. If $A_l > 0$, the sequence y_k^+ of pulse points is increasing strictly and additionally will be free from more pulse action only after limited time pulse effects.

Method 2. The asymptotic stability of boundary order-1 periodic solution can also be discussed directly from Poincaré map portrayed in (47). Let $\upsilon = 0$; then,

$$\psi(y_i^+) = -\frac{a}{b}W\left[-\frac{b}{a}y_i^+\left(\exp\left(-\frac{b}{a}y_i^+ + \frac{A_l}{a}\right)\right)\right]. \tag{72}$$

Taking the derivative of (72), we get

$$\begin{aligned}\left.\frac{d\psi(y_i^+)}{\mathrm{d}y_i^+}\right|y_i^+ = y^* &= \left.\frac{d}{\mathrm{d}y_i^+}\right|_{y_i^+ = y^*}\left(-\frac{a}{b}W\left[-\frac{b}{a}y_i^+\left(\exp\left(-\frac{b}{a}y_i^+ + \frac{A_l}{a}\right)\right)\right]\right) \\ &= \frac{-a/bW\left[-b/ay^*\left(\exp\left(-b/ay^* + A_l/a\right)\right)\right]}{1 + W\left[-b/ay^*\left(\exp\left(-b/ay^* + A_l/a\right)\right)\right]}\left(1/y^* - b/a\right) = h(y^*).\end{aligned} \tag{73}$$

The boundary order-1 periodic solution is stable $\Leftrightarrow |h(y^*)| < 1$. By utilizing the limit of $h(y^*)$, we get

$$\lim_{y^* \longrightarrow 0} h(y^*) = e^{A_l/a}. \tag{74}$$

This denotes that if $y^* \longrightarrow 0$, then $|h(y^*)| < 1$ for $A_l < 0$, and hence $(x^T(t), 0)$ is asymptotically stable.

In the following, we show the global attractivity of the boundary order-1 periodic solution $(x^T(t), 0)$. Let $p_0^+ = (\mathrm{AT}(1 - P_{\mathrm{AT}})/\theta_1 + a\theta_2, y_1^+) \in L_3$ and $p_1 = (\mathrm{AT}/\theta_1 + a\theta_2, y_2) \in L_2$ be the points of the same trajectory; then,

$$A_l = d\ln(1 - P_{\mathrm{AT}}) + c\frac{\mathrm{AT}}{\theta_1 + a\theta_2}P_{\mathrm{AT}} = a\ln\frac{y_2}{y_1^+} - b(y_2 - y_1^+). \tag{75}$$

Let $A_l \neq 0$; then, from (75), it is clear that $y_2 \neq y_1^+$. If $f(y) = a\ln y - by$, then $f(y) = a/y - b$. This indicates that if $y < a/b$, then $f(y)$ is monotonically increasing.

If $A_l < 0$, then $a\ln y_2/y_1^+ - b(y_2 - y_1^+) < 0$. Since $v = 0$, the inequality becomes $a\ln y_2/y_1 - b(y_2 - y_1) < 0$. This shows that $y_2 < y_1$. Therefore, *if* $A_l \leq 0$, then the impulsive sequence $\{y_k^+\}_{k=0}^{\infty}$ is monotonically decreasing and $\lim_{k\longrightarrow\infty} y_k^+ = y^*$. These kinds of information affirm that the boundary order-1 periodic solution is globally attractive. In the same way as above, we can prove that if $A_l > 0$, then $y_2 > y_1$. Therefore, the sequence y_k^+ will be free from impulsive effect after finite time pulse actions, as shown in Figure 2(b). Hence, from all the above outcomes, it can be concluded that if $A_l < 0$, then the boundary order-1 periodic solution, i.e., $(x^T(t), 0)$, is globally asymptotically stable.

The numerical calculation in Figure 2(a) shows that if $A_l < 0$, then the boundary order-1 periodic solution is stable while Figure 2(b) confirms that if $A_l \geq 0$, then it is unstable. □

7. Existence of Order-1 Periodic Solution

In this section, we will discuss and analyze the order-1 periodic solution for system (1) when $v > 0$.

Theorem 4. *For Case* $(A)(i)(or(ii))$*, the fixed point of Poincaré map* $\psi(y_i^+)$ *exists, and therefore an order-1 periodic solution exists for system (1).*

Proof. For Case $(A)(i)$, the trajectory Γ_1 is tangent to the curve Γ_{PS} at point (x_T, y_T) and intersects the curve Γ_{IS} at lower point G_2. If $\psi(y_T) = y_{G_2^+} = y_T$, then the curve $\widehat{TG_2}$ forms an order-1 periodic solution for system (1).

For Case $(A)(i)$, if $y_{G_2^+} > y_T$ or $y_{G_2^+} < y_T$, then the solution originating from the point G_2^+ touches the curve Γ_{PS} at a point $G_3 = (x_{G_3}, y_{G_3})$ with $y_{G_3} < y_{G_2}$. The pulse action is applied and the point G_3 maps to a point $G_3^+ = (x_{G_3^+}, y_{G_3^+})$, and $y_{G_3^+} = F(y_{G_3})$. For Case $(A)(i)$, F is increasing on $[0, y_{G_2}]$. Therefore, $y_{G_3^+} = \psi(y_{G_2^+})$ satisfies the inequality

$$\psi\left(y_{G_2^+}\right) < y_{G_2^+}. \tag{76}$$

The point $\psi_v(\mathrm{AT}(1 - P_{\mathrm{AT}})/\theta_1 + a\theta_2, v)$ being the lowest impulsive point satisfies

$$\psi(v) > v. \tag{77}$$

Inequalities (17) and (18) confirm that a fixed point of the Poincaré map exists, and therefore an order-1 periodic solution exists for system (1).

For Case $(A)(ii)$, F is decreasing on $[0, y_{G_2}]$. If $y_{G_2^+} > y_T$ or $y_{G_2^+} < y_T$, we get

$$\psi\left(y_{G_2^+}\right) > y_{G_2^+}. \tag{78}$$

Moreover, the highest impulsive point is $\psi_v(\mathrm{AT}(1 - P_{\mathrm{AT}})/\theta_1 + a\theta_2, v)$, and we get

$$\psi(v) < v. \tag{79}$$

Inequalities (19) and (20) confirm that there exists a fixed point for the Poincaré map, and therefore an order-1 periodic solution exists for system (1). This completes the proof. □

Theorem 5. *For Case* $(A)(iii)$*, the fixed point of Poincaré map* $\psi(y_i^+)$ *exists, and therefore an order-1 periodic solution exists for system (1).*

Proof. If $y_{G_2^+} = y_T$, then the curve $\widehat{TG_2}$ forms an order-1 periodic solution for the problem given in system (1). If $y_{G_2^+} \neq y_T$, then the following two cases are taken into consideration.

$$(1)\ y_{G_2^+} \geq v,\ (2)\ y_{G_2^+} < v. \tag{80}$$

For Case (1), if $y_{G_2^+} > y_T$, then we can write

$$\psi(y_T) > y_T. \tag{81}$$

As G_2^+ is the lowest impulsive point, it satisfies

$$\psi\left(y_{G_2^+}\right) < y_{G_2^+}. \tag{82}$$

Thus, inequalities (21) and (22) confirm that we can find a fixed point of Poincaré map $\psi(y_i^+)$.

If $y_{G_2^+} < y_T$, then we can write

$$\psi(y_T) < y_T. \tag{83}$$

Moreover, if G^+ is the least impulsive point, then it leads to the following:

$$\psi(y_{G^+}) \geq y_{G^+}. \tag{84}$$

Thus, the above two inequalities (83) and (84) confirm that there exists a fixed point of Poincare map $\psi(y_i^+)$.

For Case (2), if $y_{G_2^+} > y_T$, then $\psi(y_T) > y_T$. On the other hand, if the highest impulsive point is $\psi_v(\mathrm{AT}(1 - P_{\mathrm{AT}})/\theta_1 + a\theta_2, v)$, then $\psi(v) < v$. The above two inequalities affirm that there exists a fixed point of the Poincaré map $\psi(y_i^+)$.

If $y_{G_2^+} < y_T$, then $\psi(y_T) < y_T$. Moreover, as G^+ is the least impulsive point, we get $\psi(y_{G^+}) \geq y_{G^+}$. It confirms that there exists a fixed point for the map shown by $\psi(y_i^+)$, and hence an order-1 periodic solution exists for system (1). □

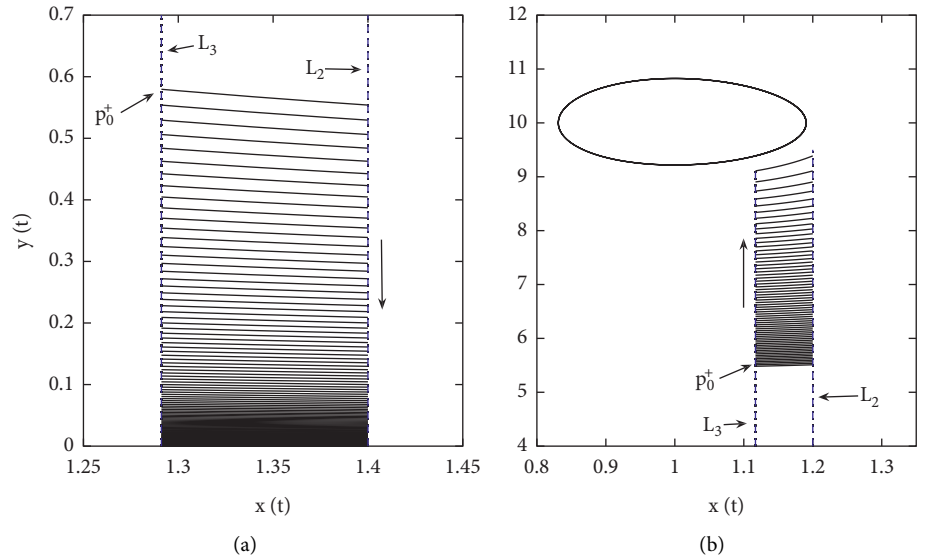

FIGURE 2: (a) The stable boundary order-1 periodic solution where $L_2 = 1.4$ and $A_l = -0.050, c = 0.50, d = 1.20$. (b) The unstable boundary order-1 periodic solution with $L_2 = 1.20$ and $A_l = 0.0030, d = 0.20, c = 0.20$. The rest of the parameter values are fixed with $a = 1, \delta = 0.3, b = 0.1, \alpha = 4, \beta = 1, \upsilon = 0$.

Theorem 6. *For Case $(B)(i)(or(ii))$, if $y_{S^+} > y_{K_1}$, then the fixed point of Poincaré map $\psi(y_i^+)$ exists, and therefore an order-1 periodic solution exists for system (1).*

Proof. For Case $(B)(i)$, we know that there exists a curve Γ_2, which is tangent to Γ_{IS} at point $S = (x_S, y_S)$ and intersects the curve Γ_{PS} at two points K_1 and K_2. If $y_{S^+} = y_{K_1}$, then the curve $\widehat{K_1 S}$ forms an order-1 periodic solution for the problem stated in (1).

Further, for Case $(B)(i)$, if $y_{S^+} > y_{K_1}$, then the point demoted by S^+ lies above the point K_1, and we get

$$\psi\left(y_{K_1}\right) > y_{K_1}. \tag{85}$$

In addition, the solution initiating from the point S^+ meets the curve Γ_{IS} at a point S_1 which lies below the point S, i.e., $y_{S_1} < y_S$. As F is increasing on $[0, y_S]$, we have $F(y_{S_1}) < F(y_S)$, i.e., $y_{S_1}^+ < y_S^+$. All the above results affirm that the Poincaré map for Case $(B)(i)$ satisfies

$$\psi\left(y_{S^+}\right) < y_{S^+}. \tag{86}$$

Inequalities (25) and (26) confirm that a fixed point in (y_{K_1}, y_{T^+}) will exist. Hence, an order-1 periodic solution exists for problem (1).

If $y_{S^+} < y_{K_1}$, then after a one time impulsive effect, the solution will directly map to the interval $[\upsilon, y_{S^+}]$. Thus, if $y_{K_2} \geq \upsilon$, then according to inequality (1), any trajectory originating from y^+ with $\upsilon \leq y^+ \leq y_{K_2}$ will intersect the curve Γ_{IS} and experience a limited time of pulse actions and at last enter into Int Γ_2 and will be free from more pulse action. If $y_{K_2} < \upsilon < y_{S^+}$, then each solution curve of problem (1) will map to the Int Γ_2 after a one time impulsive effect. Hence, if $y_{S^+} < y_{K_1}$, then a fixed point does not exist.

For Case (B) (ii), if $y_{S^+} > y_{K_1}$, then $\psi(y_{K_1}) > y_{K_1}$. We also know that the function F is decreasing on $[0, y_S]$. So, the solution y^+ initiating from $[0, y_{K_2}] \cup [y_{K_1}, \theta_1 + a\theta_2/b\theta_2 + b\theta_2\upsilon/b\theta_2 + \beta(\theta_1 + a\theta_2))$ will map to the interval $[y_{S^+}, \upsilon]$ after a one time impulsive effect. Therefore, the trajectory originating from the point $\psi_\upsilon(\mathrm{AT}(1 - P_{\mathrm{AT}})/\theta_1 + a\theta_2, \upsilon)$ will satisfy $\psi(\upsilon) < \upsilon$. From the above inequalities, it follows that the fixed point exists in the interval (y_{K_1}, υ). □

Theorem 7. *For Case $(B)(iii)$, if $y_{S^+} > y_{K_1}$, then the fixed point of Poincaré map $\psi(y_i^+)$ exists, and therefore an order-1 periodic solution exists for system (1).*

Proof. If $y_{S^+} = y_{K_1}$, then for system (1), the curve $\widehat{K_1 S}$ forms an order-1 periodic solution. If $y_{S^+} \neq y_{K_1}$, then we consider the following two cases.

$$(1)\ y_{S^+} \geq \upsilon,\ (2)\ y_{S^+} < \upsilon. \tag{87}$$

For Case (1), if $y_{T^+} > y_{K_1}$, then $\psi(y_{K_1}) > y_{K_1}$. Moreover, according to the exact domain of the Poincaré map $\psi(y_i^+)$, the impulsive point S_1^+ of S^+ lies below the point S^+, i.e., $S_1^+ < S^+$ for $y_{S^+} \geq \upsilon$. Therefore, inequality $\psi(y_{S^+}) < y_{S^+}$ is true, which shows that the fixed point exists in the interval $[y_{K_1}, y_{S^+}]$.

If $y_{S^+} < y_{K_1}$, then applying the same techniques as those given in Theorem 6, it can easily be shown there must exist a finite number of pulse effects for any solution of system (1). Furthermore, the solution enters into Int Γ_2 and becomes free from more pulse actions.

For Case (2), if $y_{S^+} > y_{K_1}$, then $\psi(y_{K_1}) > y_{K_1}$ holds true. We also know that the highest impulsive point is $\psi_\upsilon(\mathrm{AT}(1 - P_{\mathrm{AT}})/\theta_1 + a\theta_2, \upsilon)$ because $y_{S^+} < \upsilon$. Therefore, we get $\psi(\upsilon) < \upsilon$, and hence the theorem is true.

If $y_{S^+} < y_{K_1}$, then any trajectory of system (1) tends into Int Γ_2 only after finite pulse effects. This completes the proof. □

8. Stability of Order-1 Periodic Solution

The monotonicities of Poincaré map $\psi(y_i^+)$ and existence of its fixed point were discussed in previous sections. Now, based on these, we will discuss the stability of fixed point of Poincaré map $\psi(y_i^+)$ for system (1).

Theorem 8. *For Case $(A)(i)$, if the fixed point of Poincaré map $\psi(y_i^+)$ is unique and one of the following two conditions is satisfied, then the corresponding fixed point denoted by y^* is stable globally.*

(a) If $\psi(y_T) < y_T$.

(b) If $\psi(y_T) > y_T$ and $\psi^2(y_i^+) > y_i^+$ for $y_i^+ \in [y_T, y^*)$.

Proof. From Theorem 4, we know that for Case $(A)(i)$, the fixed point of Poincaré map $\psi(y_i^+)$ exists. Let the fixed point y^* be unique; then, the global stability can be discussed as follows:

(a) If $\psi(y_T) < y_T$, then $y_i^+ < \psi(y_i^+) < y^*$ for all $y_i^+ \in [0, y^*)$. This means that as j increases, $\psi^j(y_i^+)$ increases monotonically and satisfies $\lim_{j\longrightarrow+\infty} \psi^j(y_i^+) = y^*$. If $y_i^+ \in (y^*, \theta_1 + a\theta_2/b\theta_2 + b\theta_2 v/b\theta_2 + \beta(\theta_1 + a\theta_2)]$, then we take two cases. (1) If $y_i^+ \in (y^*, y_T]$, then according to the relation $y^* < \psi(y_i^+) < y_i^+$, $\psi(y_i^+)$ decreases monotonically, i.e., $y^* < \psi^j(y_i^+) < \psi^{j-1}(y_i^+)$ for all $j \geq 1$ and we get $\lim_{j\longrightarrow+\infty} \psi^j(y_i^+) = y^*$. (2) If $y_i^+ \in (y_T, \theta_1 + a\theta_2/b\theta_2 + b\theta_2 v/b\theta_2 + \beta(\theta_1 + a\theta_2))$, then $\psi(y_i^+) \in (0, y_T)$ and $\lim_{j\longrightarrow+\infty} \psi^{1+j}(y_i^+) = y^*$. Therefore, the conclusion in (a) is true.

(b) If $\psi(y_T) > y_T$, then we take three intervals: (1) $y_i^+ \in [y_T, y^*)$; (2) $y_i^+ \in [0, y_T)$; (3) $y_i^+ \in (y^*, \theta_1 + a\theta_2/b\theta_2 + b\theta_2 v/b\theta_2 + \beta(\theta_1 + a\theta_2))$. For interval (1), since $y_T \leq y_i^+ < y^*$ and Poincaré map $\psi(y_i^+)$ is monotonically decreasing in this interval, it is easy to get $(y_T) \geq \psi(y_i^+) > y^*$. At the same time, by using the second condition $\psi^2(y_i^+) > y_i^+$, we get $y_i^+ < \psi^2(y_i^+) < y^*$. This means that for all $j \geq 1$, $\psi^{2(j-1)}(y_i^+) < \psi^{2j}(y_i^+) < y^*$. This shows that $\psi^{2j}(y_i^+)$ increases monotonically, and $\lim_{j\longrightarrow+\infty} \psi^{2j}(y_i^+) = y^*$.

For intervals (2) and (3), using the same method as those in (1), we can prove that there must exist $n \geq 1$ such that $\psi^n(y_i^+) \in [y_T, y^*]$, and hence the fixed point of Poincaré map $\psi(y_i^+)$ is globally stable under conditions (2) and (3). This completes the proof. □

Theorem 9. *For Case $(A)(ii)$, if the fixed point y^* of Poincaré map $\psi(y_i^+)$ is unique and one of the following two conditions is true, then y^* is globally stable.*

(a) If $\psi(y_T) > y_T$.

(b) If $\psi(y_T) < y_T$ and $\psi^2(y_i^+) < y_i^+$ for $y_i^+ \in (y^*, y_T]$.

Proof. Theorem 4 shows that for Case (A)(ii), there exists a fixed point of the map $\psi(y_i^+)$. Assuming that the fixed point is unique, we have the following conclusions regarding its stability:

(a) From Theorem 2, it is clear that the Poincaré map is monotonically increasing in the interval $[y_T, \theta_1 + a\theta_2/b\theta_2 + b\theta_2 v/b\theta_2 + \beta(\theta_1 + a\theta_2))$ and monotonically decreasing in the interval $[0, y_T]$. If $\psi(y_T) > y_T$, then the fixed point satisfies $y^* > y_T$ for any $y_i^+ \in [y_T, y^*)$ and $\psi^{j_1}(y_i^+)$ increases with the increasing value of j_1 such that $\lim_{j\longrightarrow+\infty} \psi^{j_1}(y_i^+) = y^*$ for all $y_i^+ \in (y^*, \theta_1 + a\theta_2/b\theta_2 + b\theta_2 v/b\theta_2 + \beta(\theta_1 + a\theta_2))$. $\psi^{j_2}(y_i^+)$ decreases as j_2 increases, and $\lim_{j\longrightarrow+\infty} \psi^{j_2}(y_i^+) = y^*$.

For all $y_i^+ \in (0, y_T)$, there is $\psi(y_i^+) \in (y_T, \theta_1 + a\theta_2/b\theta_2 + b\theta_2 v/b\theta_2 + \beta(\theta_1 + a\theta_2))$; therefore, $\lim_{j\longrightarrow+\infty} \psi^{1+j_1}(y_i^+) = y^*$ or $\lim_{j\longrightarrow+\infty} \psi^{1+j_2}(y_i^+) = y^*$. In summary, the only fixed point y^* is globally stable.

(b) The Poincaré map $\psi(y_i^+)$ is monotonically decreasing in the interval $[0, y_T]$, and for $y_i^+ \in (y^*, y_T]$, the condition $\psi^2(y_i^+) < y_i^+$ is satisfied. So, it is easy to get $y^* < \psi^4(y_i^+) < \psi^2(y_i^+)$. By induction, there is a relation $y^* < \psi^{2j}(y_i^+) < \psi^{2(j-1)}(y_i^+)$ for all $j \geq 1$. This shows that $\psi^{2j}(y_i^+)$ monotonically decreases with increasing value of j, and $\lim_{j\longrightarrow+\infty} \psi^{2j}(y_i^+) = y^*$. In addition, for all $y_i^+ \in (0, y^*) \cup (y_T, \theta_1 + a\theta_2/b\theta_2 + b\theta_2 v/b\theta_2 + \beta(\theta_1 + a\theta_2))$, there must exist $l \geq 1$ such that $\psi^l(y_i^+) \in (y^*, y_T]$, and hence $\lim_{j\longrightarrow+\infty} \psi^{l+2j}(y_i^+) = y^*$. □

Theorem 10. *For Case $(A)(iii)$, if the fixed point y^* is unique and one of the following conditions is true, then it is globally stable.*

(a) If $\psi(y_{n_i}) > y_{n_i}$ $i = 1, 2$.

(b) If $\psi(y_{n_i}) < y_{n_i}$ $i = 1, 2$, and $\psi^2(y_i^+) < y_i^+$ for all $y_i^+ \in (y^*, y_{n_2}]$.

(c) If $\psi(y_T) > y_T$, $\psi(y_{n_2}) > y_{n_2}$, and $\psi(y_{n_1}) < y_{n_1}$, for $y_i^+ \in (y^*, y_{n_1}]$ when $y^* < \psi^2(y_i^+) < y_i^+$.

(d) If $\psi(y_T) < y_T$, $\psi(y_{n_2}) > y_{n_2}$, and $\psi(y_{n_1}) < y_{n_1}$.

Proof. Theorem 5 shows that there exists a fixed point of Poincaré map $\psi(y_i^+)$ for Case (A)(iii). Moreover, if y^* is unique, then its global stability can be described as follows:

(a) If $\psi(y_{n_i}) > y_{n_i}$ for $i = 1, 2$, then we take three intervals: (1) $[y_{n_1}, y^*)$; (2) $(y^*, \theta_1 + a\theta_2/b\theta_2 + b\theta_2 v/b\theta_2 + \beta(\theta_1 + a\theta_2))$; (3) $(0, y_{n_1})$. For all $y_i^+ \in [y_{n_1}, y^*)$, we get $y_i^+ < \psi(y_i^+) < y^*$. The Poincaré map $\psi(y_i^+)$ is monotonically increasing in the interval $[y_{n_1}, \theta_1 + a\theta_2/b\theta_2 + b\theta_2 v/b\theta_2 + \beta(\theta_1 + a\theta_2))$, and $\psi(y_i^+) < \psi^2(y_i^+) < y^*$. By induction, we get $\psi^{j-1}(y_i^+) < \psi^j(y_i^+) < y^*$ for all $j \geq 1$, which means that $\psi^j(y_i^+)$ monotonically increases as j increases, and $\lim_{j\longrightarrow+\infty} \psi^j(y_i^+) = y^*$, $y_i^+ \in [y_{n_1}, y^*)$.

For all $y_i^+ \in (y^*, \theta_1 + a\theta_2/b\theta_2 + b\theta_2 v/b\theta_2 + \beta(\theta_1 + a\theta_2))$, we get $y^* < \psi(y_i^+) < y_i^+$. From the

monotonicity of $\psi(y_i^+)$, we have $y^* < \psi^2(y_i^+) < \psi(y_i^+)$, which means that $\psi^j(y_i^+)$ decreases with increasing value of j and $\lim_{j\longrightarrow+\infty}\psi^j(y_i^+) = y^*$ for all $y_i^+ \in (y^*, \theta_1 + a\theta_2/b\theta_2 + b\theta_2 v/b\theta_2 + \beta(\theta_1 + a\theta_2))$. For all $y_i^+ \in (0, y_{n_1})$, it is easy to get $\psi(y_i^+) \in (y_{n_1}, \theta_1 + a\theta_2/b\theta_2 + b\theta_2 v/b\theta_2 + \beta(\theta_1 + a\theta_2))$, and according to the previous conclusion, we get $\lim_{j\longrightarrow+\infty}\psi^{1+j}(y_i^+) = y^*$. Therefore, the result in Case (a) is true.

(b) If $\psi(y_{n_i})) < y_{n_i}$ for $i = 1, 2$, then we take two cases: (1) $y_i^+ \in (y^*, y_{n_2}]$; (2) $y_i^+ \in (0, y^*) \cup (y_{n_2}, \theta_1 + a\theta_2/b\theta_2 + b\theta_2 v/b\theta_2 + \beta(\theta_1 + a\theta_2))$. For all $y_i^+ \in (y^*, y_{n_2}]$ and according to the monotonicity of the Poincaré map, $\psi(y_i^+)$ satisfies $\psi^2(y_i^+) < y_i^+$. From this, it is easy to get $y^* < \psi^4(y_i^+) < \psi^2(y_i^+)$. By induction, the inequality $y^* < \psi^{2j}(y_i^+) < \psi^{2(j-1)}(y_i^+)$ for all $j \geq 1$ holds, which means that as j increases, the mapping $\psi^{2j}(y_i^+)$ monotonically decreases, and $\lim_{j\longrightarrow+\infty}\psi^{2j}(y_i^+) = y^*$ for all $y_i^+ \in (y^*, y_{n_2}]$. For all $y_i^+ \in (0, y^*) \cup (y_{n_2}, +\infty)$, there exists $k \geq 1$, such that $\psi^k(y_i^+) \in [y^*, y_{n_2})$. From this, we get $\lim_{j\longrightarrow+\infty}\psi^{k+2j}(y_i^+) = y^*$ for all $y_i^+ \in (0, y^*) \cup (y_{n_2}, \theta_1 + a\theta_2/b\ \ \theta_2 + b\theta_2 v/b\theta_2 + \beta(\theta_1 + a\theta_2))$. All the above conclusions indicate that Case (b) is true.

(c) We again take two conditions: (1) $y_i^+ \in (y^*, y_{n_1}]$; (2) $y_i^+ \in (0, y^*) \cup (y_{n_1}, \theta_1 + a\theta_2/b\theta_2 + b\theta_2 v/b\theta_2 + \beta(\theta_1 + a\theta_2))$. For all $y_i^+ \in (y^*, y_{n_1}]$, the Poincaré map $\psi(y_i^+)$ is monotonically decreasing, and the inequality $y^* < \psi^2(y_i^+) < y_i^+$ is satisfied. We can easily get the relationship $y^* < \psi^4(y_i^+) < \psi^2(y_i^+)$, and by induction, $y^* < \psi^{2j}(y_i^+) < \psi^{2(j-1)}(y_i^+)$ for all $j \geq 1$. This means that as j increases, the mapping $\psi^{2j}(y_i^+)$ monotonically decreases, and $\lim_{j\longrightarrow+\infty}\psi^{2j}(y_i^+) = y^*$. For all $y_i^+ \in (0, y^*) \cup (y_{n_1}, +\infty)$, there must exist $l \geq 1$, such that $\psi^l(y_i^+) \in [y^*, y_{n_1}]$. Therefore, we get $\lim_{j\longrightarrow+\infty}\psi^{l+2j}(y_i^+) = y^*$ for all $y_i^+ \in (0, y^*) \cup (y_{n_1}, \theta_1 + a\theta_2/b\theta_2 + b\theta_2 v/b\theta_2 + \beta(\theta_1 + a\theta_2))$, which means that Case (c) is true.

(d) If the conditions given in statement are satisfied, we consider two intervals: (1) $y_i^+ \in [y_{n_2}, y_T]$; (2) $y_i^+ \in (0, y_{n_2}) \cup (y_T, \theta_1 + a\ \ \theta_2/b\theta_2 + b\theta_2 v/b\theta_2 + \beta(\theta_1 + a\theta_2))$. If $y_i^+ \in [y_{n_2}, y_T]$, then according to the monotonicity of the Poincaré map $\psi(y_i^+)$, $\psi^{j_1}(y_i^+)$ monotonically increases as j_1 increases, and $\lim_{j\longrightarrow+\infty}\psi^{j_1}(y_i^+) = y^*$. If $y_i^+ \in (y^*, y_T]$, then $\psi^{j_2}(y_i^+)$ monotonically decreases as j_2 increases, and $\lim_{j\longrightarrow+\infty}\psi^{j_2}(y_i^+) = y^*$. For all $y_i^+ \in (0, y_{n_2}) \cup (y_T, \theta_1 + a\theta_2/\ b\theta_2 + b\theta_2 v/\ b\theta_2 + \beta(\theta_1 + a\theta_2))$, it is easy to know that there must exist a positive integer k, such that $\psi^k(y_i^+) \in [y_{n_2}, y_T]$, and at the same time, $\lim_{j\longrightarrow+\infty}\psi^{k+j_1}(y_i^+) = y^*$ or $\lim_{j\longrightarrow+\infty}\psi^{k+j_2}(y_i^+) = y^*$. Hence, the Case (d) is true. □

Theorem 11. *For Case $(B)(i)$, if $\psi(y_{K_1}) > y_{K_1}$, then the fixed point y^* of Poincaré map $\psi(y_i^+)$ is globally asymptotically stable provided that $\psi^2(y_i^+) > y_i^+$ for all $y_i^+ \in [y_{K_1}, y^*)$.*

Proof. From Theorem 6, we know that for Case $(B)(i)$, a fixed point of Poincaré map $\psi(y_i^+)$ exists.

According to the inequality given in Lemma 3, $\psi(y_i^+) > y_i^+$ for all $y_i^+ \in (0, y_{K_2})$. At the same time, the inequality $\psi(0) = v > 0$ is satisfied. So, the fixed point y^* does not lie in the interval $[0, y_{K_2}]$. This shows that the unique fixed point belongs to the interval $[y_{K_1}, \theta_1 + a\theta_2/b\theta_2 + b\theta_2 v/b\theta_2 + \beta(\theta_1 + a\theta_2))$.

If $y_{K_1} \leq y_i^+ < y^*$, then from the monotonicity of the mapping $\psi(y_i^+)$, we get $\psi(y_{K_1}) \geq \psi(y_i^+) > y^*$. By applying the inequality $\psi^2(y_i^+) > y_i^+$ for all $y_i^+ \in [y_{K_1}, y^*)$, we get $y_i^+ < \psi^2(y_i^+) < y^*$. By induction, there exists a relationship $\psi^{2(j-1)}(y_i^+) < \psi^{2j}(y_i^+) < y^*$ for all $j \geq 1$. This means that as j increases, $\psi^{2j}(y_i^+)$ increases monotonically, and hence $\lim_{j\longrightarrow+\infty}\psi^{2j}(y_i^+) = y^*$. □

Theorem 12. *For Case $(B)(ii)$, if $\psi(y_{K_1}) > y_{K_1}$, then the fixed point of Poincaré map $\psi(y_i^+)$ is globally stable.*

Proof. From Theorem 6, there exists a fixed point of Poincaré map $\psi(y_i^+)$ for Case (B)(ii). Using the same method as in Theorem 11, there is no fixed point on the interval $[0, y_{K_2}]$, and y^* is located in the interval $(y_{K_1}, \theta_1 + a\theta_2/b\theta_2 + b\theta_2 v/b\theta_2 + \beta(\theta_1 + a\theta_2))$. Moreover, under the uniqueness of y^*, the global stability can be described as follows.

For Case (B)(ii), the Poincaré map $\psi(y_i^+)$ is monotonically decreasing in the interval $[0, y_{K_2}]$ and monotonically increasing in the interval $[y_{K_1}, \theta_1 + a\theta_2/b\theta_2 + b\theta_2 v/b\theta_2 + \beta(\theta_1 + a\theta_2))$. If $y_i^+ \in [y_{K_1}, y^*)$, then according to the relationship $y_i^+ < \psi(y_i^+) < y^*$, it is obvious that $\psi^j(y^+)$ increases monotonically towards y^* as j increases, i.e., $\lim_{j\longrightarrow+\infty}\psi^j(y_i^+) = y^*$. For all $y_i^+ \in (y^*, \theta_1 + a\theta_2/b\theta_2 + b\theta_2 v/b\theta_2 + \beta(\theta_1 + a\theta_2))$, according to the relationship $y^* < \psi(y_i^+) < y_i^+$ and properties of Poincaré map $\psi(y_i^+)$, we know that $\psi^j(y_i^+)$ monotonically decreases with the increasing value of j, and $\lim_{j\longrightarrow+\infty}\psi^j(y_i^+) = y^*$.

If $y_i^+ \in [0, y_{K_2}]$, then there must exist some $l \geq 1$ such that $\psi(y_i^+) \in [y_{K_1}, \theta_1 + a\theta_2/b\theta_2 + b\theta_2 v/b\theta_2 + \beta(\theta_1 + a\theta_2))$, and therefore $\lim_{j\longrightarrow+\infty}\psi^{1+j}(y_i^+) = y^*$. Hence, the result in Theorem 12 is correct. □

Theorem 13. *For Case $(B)(iii)$, if $\psi(y_{K_1}) > y_{K_1}$, then the unique fixed point y^* of Poincaré map $\psi(y_i^+)$ exists. If one of the conditions (a) and (b) given below is true, then y^* is globally stable.*

(a) If $\psi(y_{N_i}) > y_{N_i}$ $i = 1, 2$.

(b) If $y_{K_1} \leq \psi(y_{N_2}) = \psi(y_{N_1}) \leq y_{N_1}$, and $\psi^2(y_i^+) > y_i^+$ for all $y_i^+ \in [y_{K_1}, y^*)$.

Proof. For Case (B)(iii), if $\psi(y_{K_1}) > y_{K_1}$, then from Lemma 3 and Theorem 7, we know that Poincaré mapping $\psi(y_i^+)$ has at least one fixed point y^* belonging to the interval $[y_{K_1}, \theta_1 + a\theta_2/b\theta_2 + b\theta_2 v/b\theta_2 + \beta(\theta_1 + a\theta_2))$. Under the uniqueness of y^*, the global stability can be demonstrated as follows:

(a) If $\psi(y_{N_i}) > y_{N_i}$ $i = 1, 2$, then only y^* exists in the interval $[y_{N_1}, \theta_1 + a\theta_2/b\theta_2 + b\theta_2 v/b\theta_2 + \beta(\theta_1 + a\theta_2))$. From Theorem 2, we can see that Poincaré map $\psi(y_i^+)$ is monotonically increasing in the interval $[y_{N_1}, \theta_1 + a\theta_2/b\theta_2 + b\theta_2 v/b\theta_2 + \beta(\theta_1 + a\theta_2))$. For any $y_i^+ \in [y_{N_1}, y^*)$, we get $y_i^+ < \psi(y_i^+) < y^*$, which shows that $\psi^j(y_i^+)$ for $j \geq 1$ increases monotonically, and $\lim_{j\longrightarrow+\infty}\psi^j(y_i^+) = y^*$. For any $y_i^+ \in (y^*, \theta_1 + a\theta_2/b\theta_2 + b\theta_2 v/b\theta_2 + \beta(\theta_1 + a\theta_2)]$, we get the relation $y^* < \psi(y_i^+) < y_i^+$. Therefore, from the monotonicity of $\psi(y_i^+)$, $\psi^j(y_i^+)$ monotonically decreases with increasing value of j, and we get $\lim_{j\longrightarrow+\infty}\psi^j(y_i^+) = y^*$. For all $y_i^+ \in [0, y_{K_2}] \cup [y_{K_1}, y_{N_1})$, it is obvious that there exists an integer $l \geq 0$, such that $\psi^l(y_i^+) \in [y_{N_1}, \theta_1 + a\theta_2/\ b\theta_2 + b\theta_2 v/b\theta_2 + \beta(\theta_1 + a\theta_2))$. Hence, for all $y_i^+ \in [0, y_{K_2}] \cup [y_{K_1}, y_{N_1})$, we get $\lim_{j\longrightarrow+\infty}\psi^{l+j}(y_i^+) = y^*$.

All these results show that if $\psi(y_{N_i}) > y_{N_i}$ $i = 1, 2$, then the unique fixed point y^* of the mapping $\psi(y_i^+)$ is globally stable.

(b) If $y_{K_1} \leq \psi(y_{N_2}) = \psi(y_{N_1}) \leq y_{N_1}$, then combined with the inequality $\psi(y_{K_1}) > y_{K_1}$ given in the statement, it is clear that there exists only one y^* in the interval $(y_{K_1}, y_{N_1}]$. The mapping $\psi(y_i^+)$ monotonically decreases in the interval $[y_{K_1}, y^*)$, i.e., for all $y_i^+ \in [y_{K_1}, y^*)$, we have $\psi(y_{K_1}) \geq \psi(y_i^+) > y^*$. In addition, by applying the condition $\psi^2(y_i^+) > y_i^+$, we get $y_i^+ < \psi^2(y_i^+) < y^*$. Hence, we get $\psi^{2(j-1)}(y_i^+) < \psi^{2j}(y_i^+) < y^*$ for $j \geq 1$. This shows that $\psi^{2j}(y_i^+)$ monotonically increases with the increasing value of j and $\lim_{j\longrightarrow+\infty}\psi^{2j}(y_i^+) = y^*$ for all $y_i^+ \in [y_{K_1}, y^*)$.

If $y_i^+ \in (0, y_{K_2}) \cup (y^*, \theta_1 + a\theta_2/b\theta_2 + b\theta_2 v/b\theta_2 + \beta(\theta_1 + a\theta_2))$ and $y_{K_1} \leq \psi(y_{N_2}) = \psi(y_{N_1}) \leq y_{N_1}$, then there must exist $l \geq 1$ such that $\psi^l(y_i^+) \in [y_{K_1}, y^*]$. By using the same way as above, we get $\lim_{j\longrightarrow+\infty}\psi^{l+2j}(y_i^+) = y^*$ for all $y_i^+ \in [0, y_{K_2}] \cup (y^*, \theta_1 + a\theta_2/b\theta_2 + b\theta_2 v/b\theta_2 + \beta(\theta_1 + a\theta_2))$.

Therefore, if $y_{K_1} \leq \psi(y_{N_2}) = \psi(y_{N_1}) \leq y_{N_1}$ and $\psi^2(y_i^+) > y_i^+$ for all $y_i^+ \in [y_{K_1}, y^*)$, then the fixed point y^* is globally stable. □

9. Conclusions

The IPM strategy is a dynamic management system. From a mathematical perspective, this is actually an optimal control problem under multiple objectives. The IPM approach's purpose is to monitor the number of pest populations in real time and decide whether to implement a control strategy based on the size of the population. The state-dependent impulsive differential equation [20, 45–47] is needed to truly characterize the IPM strategy and the dynamic evolution of pest-natural system. Moreover, in recent years, researchers have proposed a variety of state-dependent pest-natural enemy feedback control systems.

The change rate of pest population plays an important role in state-dependent prey-predator ecological system. There are two fundamental circumstances in the previous studies which require high attention. First, the pest population is comparatively high and the change rate is little; second, the population of pest is small, but the change rate is high. A crucial issue illustrated by these two situations is that when the pest population is large, the growth rate is small or even negative at this time. In this case, even if the IPM strategy is not implemented, the number of pests may not exceed EIL. Another situation is that although the number of pests is not large, the growth rate of the pest population is very large. If the control strategy is not implemented in time, it may lead to a large outbreak of pests. Next, the IPM process needs precise checking of the pest populations, and consequently suitable integrated control strategies can be prepared. The pest killing rate should be a function of their density, whereas the releasing quantity of natural enemies should be a function of their density. Based on this, a feasible new nonlinear state-feedback system with nonlinear ratio-dependent AT is proposed.

The use of nonlinear pulse as state-dependent feedback control with nonlinear ratio-dependent AT is more reasonable and closer to reality in a biological sense, but the impulsive model becomes very difficult because of the existence of two population quantities in the control actions. By including the densities of pest and its natural enemy in controlling measures, we can develop the pest control model based on the practical importance according to the growth direction of agriculture and forestry. Corresponding analytical techniques and numerical methods were developed, the dynamic behavior of the system was examined, and the important role of the main conclusions in integrated pest control was given.

To avoid the complexity, in this paper, we proposed the simple Lotka–Volterra impulsive mathematical model. Our aim is to reveal how nonlinear pulse control with nonlinear ratio-dependent AT affects the whole dynamics and concentrate on the biological implications. The definition and properties of Poincaré map for phase-concentrated pulse points in various cases are discussed and studied. The existence, uniqueness, and global stability of boundary and interior periodic solutions of order 1 for model (1) are analyzed by using the definition of Poincaré map. In the present paper, some basic techniques were used for the qualitative analysis of nonlinear pulsed model with nonlinear ratio-depended AT, which can be widely used in the study of feedback control systems with critical conditions, such as the blood glucose-insulin regulation system.

Data Availability

The data used to support the findings of this study are included within the article.

Conflicts of Interest

The authors declare that they have no conflicts of interest.

Acknowledgments

Basem Al Alwan would like to thank the Deanship of Scientific Research at King Khalid University, Abha, K.S.A., for funding this work through a research group program under grant no. RGP.2/204/42.

References

[1] S. Tang, L. Chen, and L. Chen, "Modelling and analysis of integrated pest management strategy," *Discrete & Continuous Dynamical Systems - B*, vol. 4, no. 3, pp. 759–768, 2004.

[2] S. Tang, G. Tang, and R. A. Cheke, "Optimum timing for integrated pest management: modelling rates of pesticide application and natural enemy releases," *Journal of Theoretical Biology*, vol. 264, no. 2, pp. 623–638, 2010.

[3] S. Tang, J. Liang, Y. Tan, and R. A. Cheke, "Threshold conditions for integrated pest management models with pesticides that have residual effects," *Journal of Mathematical Biology*, vol. 66, no. 1-2, pp. 1–35, 2013.

[4] V. Lakshmikantham, D. D. Bainov, and P. S. Simeonov, *Theory of Impulsive Diferential Equations*, World Scientific, Singapore, 1989.

[5] P. Wang, W. Qin, and G. Tang, "Modelling and analysis of a host-parasitoid impulsive ecosystem under resource limitation," *Complexity*, vol. 2019, Article ID 9365293, 12 pages, 2019.

[6] S. Saha and G. Samanta, "Modeling of insect-pathogen dynamics with biological control," *Mathematical Biology and Bioinformatics*, vol. 15, no. 2, pp. 268–294, 2020.

[7] J. C. van Lenteren and J. Woets, "Biological and integrated pest control in greenhouses," *Annual Review of Entomology*, vol. 33, no. 1, pp. 239–269, 1988.

[8] L. Nie, J. Peng, Z. Teng, and L. Hu, "Existence and stability of periodic solution of a Lotka-Volterra predator-prey model with state dependent impulsive effects," *Journal of Computational and Applied Mathematics*, vol. 224, no. 2, pp. 544–555, 2009.

[9] L. Nie, Z. Teng, L. Hu, and J. Peng, "Existence and stability of periodic solution of a predator-prey model with state-dependent impulsive effects," *Mathematics and Computers in Simulation*, vol. 79, no. 7, pp. 2122–2134, 2009.

[10] Y. Tian, K. Sun, and L. Chen, "Modelling and qualitative analysis of a predator-prey system with state-dependent impulsive effects," *Mathematics and Computers in Simulation*, vol. 82, no. 2, pp. 318–331, 2011.

[11] L. Zhao, L. Chen, and Q. Zhang, "The geometrical analysis of a predator-prey model with two state impulses," *Mathematical Biosciences*, vol. 238, no. 2, pp. 55–64, 2012.

[12] T. Zhang, X. Meng, R. Liu, and T. Zhang, "Periodic solution of a pest management Gompertz model with impulsive state feedback control," *Nonlinear Dynamics*, vol. 78, no. 2, pp. 921–938, 2014.

[13] A. Mondal, A. K. Pal, and G. P. Samanta, "Analysis of a delayed eco-epidemiological pest-plant model with infected pest," *Biophysical Reviews and Letters*, vol. 14, no. 3, pp. 141–170, 2019.

[14] M. B. Thomas, "Ecological approaches and the development of "truly integrated" pest management," *Proceedings of the National Academy of Sciences*, vol. 96, no. 11, pp. 5944–5951, 1999.

[15] S. U. Karaagac, *Insecticide Resistance*, InTech Press, London, 2012.

[16] P. DeBach and D. Rosen, *Biological Control by Natural Enemies*, Cambridge University Press, Cambridge, 1991.

[17] J. Grasman, O. A. van Herwaarden, L. Hemerik, and J. C. van Lenteren, "A two-component model of host-parasitoid interactions: determination of the size of inundative releases of parasitoids in biological pest control," *Mathematical Biosciences*, vol. 169, no. 2, pp. 207–216, 2001.

[18] A. Maiti, A. K. Pal, and G. P. Samanta, "Usefulness of b of pests in tea: a mathematical model," *Mathematical Modelling of Natural Phenomena*, vol. 3, no. 4, pp. 96–113, 2008.

[19] A. Maiti, B. Patra, and G. P. Samanta, "Sterile insect release method as a control measure of insect pests: a mathematical model," *Journal of Applied Mathematics and Computing*, vol. 22, no. 3, pp. 71–86, 2006.

[20] S. Tang, Y. Xiao, and R. A. Cheke, "Multiple attractors of host-parasitoid models with integrated pest management strategies: eradication, persistence and outbreak," *Theoretical Population Biology*, vol. 73, no. 2, pp. 181–197, 2008.

[21] S. Tang, Y. Xiao, L. Chen, and R. Cheke, "Integrated pest management models and their dynamical behaviour," *Bulletin of Mathematical Biology*, vol. 67, no. 1, pp. 115–135, 2005.

[22] J. C. V. Lenteren, "Integrated pest management in protected crops," in *Integrated Pest Management*, D. Dent, Ed., pp. 311–343, Chapman & Hall, London, 1995.

[23] J. C. V. Lenteren, *Environmental Manipulation Advantageous to Natural Enemies of Pests*, V. Delucchi, Ed., pp. 123–166, Integrated Pest Management, Parasitis, Geneva, 1987.

[24] Y. N. Xiao and F. V. D. Bosch, "The dynamics of an eco-epidemic model with biological control," *Ecological Modelling*, vol. 168, no. 1-2, pp. 203–214, 2003.

[25] H. J. Barclay, "Models for pest control using predator release, habitat management and pesticide release in combination," *Journal of Applied Ecology*, vol. 19, no. 2, pp. 337–348, 1982.

[26] W. Znegui, H. Gritli, and S. Belghith, "Stabilization of the passive walking dynamics of the compass-gait biped robot by developing the analytical expression of the controlled Poincaré map," *Nonlinear Dynamics*, vol. 101, no. 8, pp. 1061–1091, 2020.

[27] W. Znegui, H. Gritli, and S. Belghith, "A new Poincaré map for investigating the complex walking behavior of the compass-gait biped robot," *Applied Mathematical Modelling*, vol. 94, pp. 534–557, 2021.

[28] H. Gritli and S. Belghith, "Walking dynamics of the passive compass-gait model under OGY-based state-feedback control: analysis of local bifurcations via the hybrid Poincaré map," *Chaos, Solitons & Fractals*, vol. 98, pp. 72–87, 2017.

[29] W. Znegui, H. Gritli, and S. Belghith, "Design of an explicit expression of the Poincaré map for the passive dynamic walking of the compass-gait biped model," *Chaos, Solitons & Fractals*, vol. 130, no. 12, 2020.

[30] H. Gritli, F. Turki, and S. Belghith, "State-feedback control via LMI approach of a 1-DOF disturbed impacting mechanical oscillator under double-side rigid constraints," in *Proceedings of the International Conference on Advanced Systems and Electric Technologies (IC ASET)*, pp. 441–448, IEEE, Hammamet, Tunisia, 22 March 2018.

[31] F. Turki, H. Gritli, and S. Belghith, "Robust position control of a two-sided 1-DoF impacting mechanical oscillator subject to an external persistent disturbance by means of a state-Feedback controller," *Complexity*, vol. 2019, Article ID 9174284, 14 pages, 2019.

[32] G. P. Samanta, "Analysis of a delayed epidemic model with pulse vaccination," *Chaos, Solitons & Fractals*, vol. 66, pp. 74–85, 2014.

[33] J. Wang, H. Cheng, X. Meng, and B. G. S. A. Pradeep, "Geometrical analysis and control optimization of a predator-prey model with multi state-dependent impulse," *Advances in Difference Equations*, vol. 2017, Article ID 252, 2017.

[34] Q. Xiao and B. Dai, "Periodic solutions generated by impulses for state-dependent impulsive differential equation," *Discrete*

Dynamics in Nature and Society, vol. 2015, Article ID 816325, 7 pages, 2015.

[35] L. Feng and Z. Liu, "An impulsive periodic predator-prey Lotka-Volterra type dispersal system with mixed functional responses," *Journal of Applied Mathematics and Computing*, vol. 45, no. 1-2, pp. 235–257, 2014.

[36] M. Kogan, "Integrated pest management: historical perspectives and contemporary developments," *Annual Review of Entomology*, vol. 43, no. 1, pp. 243–270, 1998.

[37] S. Tang and R. A. Cheke, "State-dependent impulsive models of integrated pest management (IPM) strategies and their dynamic consequences," *Journal of Mathematical Biology*, vol. 50, no. 3, pp. 257–292, 2005.

[38] Y. Tian, S. Tang, and R. A. Cheke, "Nonlinear state-dependent feedback control of a pest-natural enemy system," *Nonlinear Dynamics*, vol. 94, no. 3, pp. 2243–2263, 2018.

[39] I. U. Khan, S. Y. Tang, and B. Tang, "The state-dependent impulsive model with action threshold depending on the pest density and its changing rate," *Complexity*, vol. 2019, Article ID 6509867, 15 pages, 2019.

[40] S. H. M. J. Houben, J. M. L. Maubach, and R. M. M. Mattheij, "An accelerated Poincaré-map method for autonomous oscillators," *Applied Mathematics and Computation*, vol. 140, no. 2-3, pp. 191–216, 2003.

[41] R. Efrem, "Numerical approximation of Poincaré maps," *Romanistisches Jahrbuch*, vol. 4, no. 1, pp. 101–106, 2008.

[42] M. Henon, "On the numerical computation of Poincar maps," *Physica D: Nonlinear Phenomena*, vol. 5, no. 2-3, pp. 412–414, 1982.

[43] P. S. Simeonov and D. D. Bainov, "Orbital stability of periodic solutions of autonomous systems with impulse effect," *International Journal of Systems Science*, vol. 19, no. 12, pp. 2561–2585, 1988.

[44] D. Bainov and P. Simeonov, *Impulsive Differential Equations, Periodic Solutions and Applications, Monographs and Surveys in Pure and Applied Mathematics*, Longman Scientific and Technical, New York, 1993.

[45] S. Tang and R. A. Cheke, "Models for integrated pest control and their biological implications," *Mathematical Biosciences*, vol. 215, no. 1, pp. 115–125, 2008.

[46] J. Yang and S. Tang, "Holling type II predator-prey model with nonlinear pulse as state-dependent feedback control," *Journal of Computational and Applied Mathematics*, vol. 291, pp. 225–241, 2016.

[47] S. Y. Tang, X. W. Tan, J. Yang, and J. H. Liang, "Periodic solution bifurcation and spiking dynamics of impacting predator-prey dynamical model," *Int. J. Bif. and Chaos*, vol. 28, no. 12, 2018.